A MASTER THESIS

Plasma Enhanced Dry Reforming of Propane to Syngas over Ni- CeO_2/γ-Al_2O_3 Catalysts in DBD Reactor

LAMIA SULTANA

DEPARTMENT OF CHEMICAL AND BIOLOGICAL ENGINEERING

FACULTY OF APPLIED ENERGY SYSTEM

GRADUATE SCHOOL

JEJUNATIONAL UNIVERSITY

February, 2018

Plasma Enhanced Dry Reforming of Propane to Syngas over Ni- CeO$_2$/ γ-Al$_2$O$_3$ Catalysts in DBD Reactor

Lamia Sultana

(Supervised by Professor Young Sun Mok)

A thesis submitted in partial fulfillment of the requirement for the degree of Master of Engineering

18-12-2017

This thesis has been examined and approved

....

Thesis director

Professor Young Sun Mok, Chemical and Biological Engineering

....

Professor Young Jin Hyun, Chemical and Biological Engineering

....

Professor Heon-Ju Lee, Nuclear and Energy Engineering

Date: ....

Department of Chemical and Biological Engineering

GRADUATE SCHOOL

JEJU NATIONAL UNIVERSITY

PREAMBLE

This thesis is submitted for the degree of Master of Engineering in the Department of Chemical and Biological Engineering, Jeju National University, Korea under the supervision of Professor Dr. Young Sun Mok. No segment of this master thesis has been submitted previously for any degree at any other research organization or academic institution. According to the author's knowledge, this master thesis work is fully original unless reference is taken from others research works. Parts of this thesis have been published in two national conferences in South Korea as listed below:

Conference proceedings:

1. Lamia Sultana, M.S.P.Sudhakaran, Md. Shahinur Rahman, Md. Mokter Hossain and Young Sun Mok*, "Syngas production via dry reforming of propane over Ni supported on γ/Al_2O_3 modified with CeO_2 catalysts " KSIEC 2017, 10 to 12 May, Gwangju, Korea.

2. Lamia Sultana, M.S.P.Sudhakaran, Md. Shahinur Rahman, Md. Mokter Hossain and Young Sun Mok*, "Plasma-Catalytic Dry Reforming of Propane to Syngas over Ni- $CeO_2/ \gamma-Al_2O_3$ Catalysts in DBD Reactor" BK 2017, 24 November, Jeju, Korea.

ABBREVIATIONS

AC	Alternating current.
CAS	Chemical abstracts service.
DRP	Dry reforming of propane.
DBD	Dielectric barrier discharge.
FE-SEM	Field-emission scanning electron microscopy.
FE-SEM	Field-emission scanning electron microscopy.
FTIR	Fourier-transform infrared spectroscopy.
GC	Gas chromatography.
GHGs	Greenhouse Gas
kV	Kilovolt
LPG	Liquefied Petroleum Gas.
ppm	Parts per million
PRC	Plasma reduced catalyst.
SIE	Specific input energy.
SMR	Steam methane reforming.
Syngas	Synthesis gas (a mixture of H_2 and CO)
TRC	Thermally reduced catalyst.
TPD	Temperature programmed desorption.
TPR	Temperature programmed reduction.
TCD	Thermal conductivity detector
V_b	Breakdown voltage.
WGSR	Water-gas shift reaction.
XRD	Powder X-ray diffraction.

Appendix A

A.1 MATLAB code used to obtain QU-Lissajous Figure for Power Measurement

Dedicated To My

Parents And Beloved Husband

ACKNOWLEDGEMENTS

experimental works. I am also thankful to my junior lab mate Mr. Byeong Ju Lee for his kind cooperation in our laboratory.

I am really owed to my parents who gave birth to me in this materialistic earth and also educated me with their highest supports within limitations. Indeed, my words are powerless to express my heart-felt gratitude to my beloved husband, Md. Shahinur Rahman (PhD Research Scholar, Nuclear Engineering Physics, School of Physical, Environmental and Mathematical Sciences (PEMS), The University of New South Wales (UNSW), Australia) for his unwavering support and encouragement to my master study in Jeju National University, South Korea. Furthermore, he (my husband) taught me the initial experimental setup and characterization techniques for this research study, and finally, he helped to structure this master thesis writing with proofreading and scientific explanation for the results and discussion section.

I acknowledge the financial support of Korean Government under Brain of Korea 21+ (BK 21+) project for the master thesis research project work. Moreover, I would like to appreciate the staffs of the Chemical & Biological Engineering Department for their kindness and great help in official issues. Thus, I am very much lucky and delighted to pursue my master of engineering degree in Jeju National University, South Korea. However, I will always remember the spectacular surroundings & beautiful landscapes of the Jeju Island, South Korea, which is one of the 7 new wonders of the world announced by UNESCO.

Finally, I have to pay my earnest gratitude to almighty God who has given me the invaluable life, exciting opportunity and maximum ability to study and do research in plasma field for gathering knowledge.

<div align="right">

Lamia Sultana

2017.12.18

</div>

TABLE OF CONTENTS

LIST OF FIGURES

v

LIST OF TABLES

ABSTRACT

 Syngas (a mixture of CO and H_2) production from dry reforming of propane (DRP) over Ni-based catalyst has attained huge interests in the production of value-added oxygenated chemicals and high tech industrial applications as an environment-friendly process. A coaxial dielectric barrier discharge (DBD) reactor has been developed for DRP over Ni-CeO$_2$-γ/Al$_2$O$_3$ catalyst with 4 wt.% of cerium and nickel metals (2 wt% each). In addition, plasma-catalytic DRP has been carried out with the thermally and plasma-reduced Ni-CeO$_2$-γ/Al$_2$O$_3$ catalysts using the reactant ratio of C_3H_8/CO_2 at 1/3 at a total flow rate of 300 ml min^{-1}. After general calcination in air, the Ni-CeO$_2$-γ/Al$_2$O$_3$ catalysts were reduced by thermal and plasma-assisted process in H_2/Ar atmosphere. The catalytic activities for DRP were evaluated at 500-600°C. Thermally and plasma-reduced (H_2 and plasma-assisted) catalysts' properties before and after DRP reactions were investigated using XRD, TEM, FE-SEM, temperature programmed reduction (H_2-TPR) techniques, temperature programmed desorption (H_2-TPD, CO_2-TPD) and Raman spectroscopy. The Ni-CeO$_2$-γ/Al$_2$O$_3$ catalyst prepared by plasma reduction exhibited better catalytic performance towards H_2 production, compared with thermally reduced catalysts, which is attributed to the nickel particles' nanoconfinement within the interaction between the support and favorable metal-support as a result of plasma-assisted reduction mechanism. One of the main concerns regarding the DRP process is catalyst deactivation due to excess amount of carbon deposition. The plasma-reduced Ni-CeO$_2$-γ/Al$_2$O$_3$ catalyst for the DRP process exhibited long term stability at 600°C for anti-sintering and coke resistance with high reactivity and durability without severe deactivation as a potential catalyst.

Keywords*: Dry reforming, Plasma reduction, Dielectric barrier discharge, Ni catalysts, Catalytic activity, Synthesis gas.

CHAPTER I

INTRODUCTION

1.1 Brief Introduction from Literature Review

To date, Global warming is an alarming issue for excessive carbon dioxide (CO2) emissions in the ambient atmosphere which acts as a blanket and traps the radiated heat wave subsequently from the sun to the earth's surface, and then it warms the entire planet drastically. Therefore, the reduction of greenhouse gas emission using advanced technology is very urgent to save our lovely planet for healthy life. According to Chen et al., above 60% of the world's raw material such as natural gas is a mixture of methane gas, light hydrocarbons, and non-hydrocarbons is used for hydrogen production [1]. Over the last two decades, CO_2 reforming with hydrocarbons (methane, propane, ethane, butane, etc.) also known as dry reforming, which has received a great research interest from the angle of effective utilization of petroleum and greenhouse gas as an alternative source for the production of syngas. Syngas is one of the most important industrial feedstocks for the production of a variety of oxygenated chemicals and sulfur-free liquid fuels at a low H_2/CO ratio is so-called Fischer-Tropsch processes and its potentially serve as a fuel for more efficient energy conversion devices, such as fuel cells, petrochemical products as well as a potential reduction of greenhouse gas emissions. Inspired by the needs of alternative sources for the chemical and petrochemical industries to produce syngas, Fischer and Tropsch developed the dry (CO_2) reforming of methane (DRM) technique over various metals for the synthesis of long-chain hydrocarbons back in 1928 [2]. However, the steam methane reforming (SMR) technique is the primary source of syngas production in the industry to date, whereas the dry reforming of methane process is not well established yet in chemical and fuel industries due to lack of information. Although SMR is widely used in the industry for syngas production over the last two decades, but now it still has some drawbacks which motivate the development of other alternative reforming technologies. In addressing the aforementioned problem, non-thermal plasma technology can be considered as a leading candidate to convert greenhouse gases

1

into syngas and other valuable chemicals at a lower temperature, because highly reactive species are generated during plasma discharge which is favorable for both the initiation and propagation of chemical reactions. On the other hand, the combination of plasma technology and heterogeneous catalysts for fuel production from hydrocarbon reforming has attracted significant interest in the scientific community as the interaction of plasma induced reactive species with catalyst could result in a synergistic effect, which might create a unique way to separate the activation steps from the selective reactions [3]. Furthermore, to date, most of the ongoing research studies in syngas production domain are mainly focusing on the plasma-catalytic chemical reactions to maximize the process performance [4]. On the contrary, the main concern in the SMR is it utilizes the excess amount of water as a reactant and it requires large amounts of heat supply which leads to high process cost. Syngas production with Fischer-Tropsch (F-T) technique is the major source of hydrogen fuel production in the modern refinery processing field; however, it is a very necessary component in the present advanced chemical and petrochemical industry for different applications such as methanol, ammonia and hydrogen production. Although the SMR is a well-established technique for syngas production, then further study of DRM is aiming to achieve significant improvement in reducing CO_2 emission in our environment for healthy living with significant research findings for a proper explanation about the key reaction mechanism between plasma-catalyst. In this research study, we focused on propane (C_3H_8) instead of methane (CH_4) due to higher hydrogen content with CO_2 as an essential oxidizing agent over a heterogeneous catalyst to conduct a perfect DRP process for establishing the key reaction mechanism as an academic research.

1.2 Objectives:

- ➢ The main purpose of this research is to produce syngas (a mixture of H_2+CO) with a low H_2/CO ratio, which is favorable for the production of value-added oxygenated chemicals and liquid fuels.

➢ Secondly, to develop a suitable catalyst using a plasma process for syngas production that possesses high activity, stability and minimum coking rate during DRP.

➢ Thirdly, to reduce the reaction temperature by the combination of catalysis with plasma whilst minimizing any side reactions leading to coke formation.

1.3. Significance of Dry Reforming Research:

Syngas has huge demand as an essential fuel in chemical and petrochemical industries to date, so dry reforming of hydrocarbon for syngas production with greenhouse gas emission reduction is very necessary. However, the dry reforming of hydrocarbon is at the development stage and it is not yet commercialized in industry for practical applications. This systematic DRP research study will provide a deep theoretical knowledge in product distribution as a function of reaction ratios, reaction temperature and gas pressure. More precisely, it can be a great solution to minimize CO_2 gas emissions in our environment with syngas production for industrial applications.

1.4.The Scope of Research:

▪ To identify the side reactions as a by-product of DRP reaction.

▪ To study the effect of temperature on the catalyst in reforming reactions.

▪ To identify the effect of applied energy (voltage) on DRP process.

▪ To define the effect of catalyst (plasma reduced and thermal reduced) in dry reforming of propane.

CHAPTER II

LITERATURE REVIEW

2.1 Historical Background

Man-made greenhouse gas emissions (GHG), including CO_2, methane, nitrous oxide (N_2O), sulphur hexafluoride (SF6), chlorofluorocarbons (CFCs) and hydrochlorofluorocarbons (HCFCs) have resulted in an increase of greenhouse effect (global warming) severely whilst the large extent of radiation is trapped in the Earth's atmosphere. Alongside this, it has resulted in the increase of average global temperature, the decrease in the pH of the ocean surface and significant changes to local weather systems (global climate change) [5]. On the other hand, GHG gas emissions are also strongly related to the world population growth and consequently to the growing energy demand, evidenced by the fact that CH_4 and CO_2 emissions have resulted from the developing agriculture, natural gas process activities and fossil fuel combustions. Many research organizations are continuously working on the development of alternative technologies which will be very effective to solve the aforementioned problem.
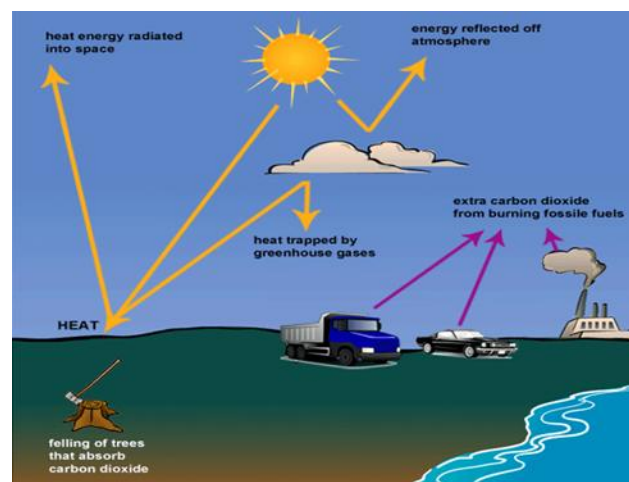
Figure.1: Schematic diagram showing the Earth's energy balance through incoming and outgoing radiation (Wikipedia).

4

South Korea pledged to reduce its greenhouse gas emissions around 37% by 2030 [6], from different industrial sectors across the country. In accordance with the Framework Act on low carbon, Green Growth Korea has been putting huge efforts to address climate change across all economic sectors and will strengthen its efforts to achieve the 2030 mitigation target. The country is among the world's top 10 carbon emitters, so any steps it takes to curb emissions are key to global efforts to combat greenhouse gases in the environment.
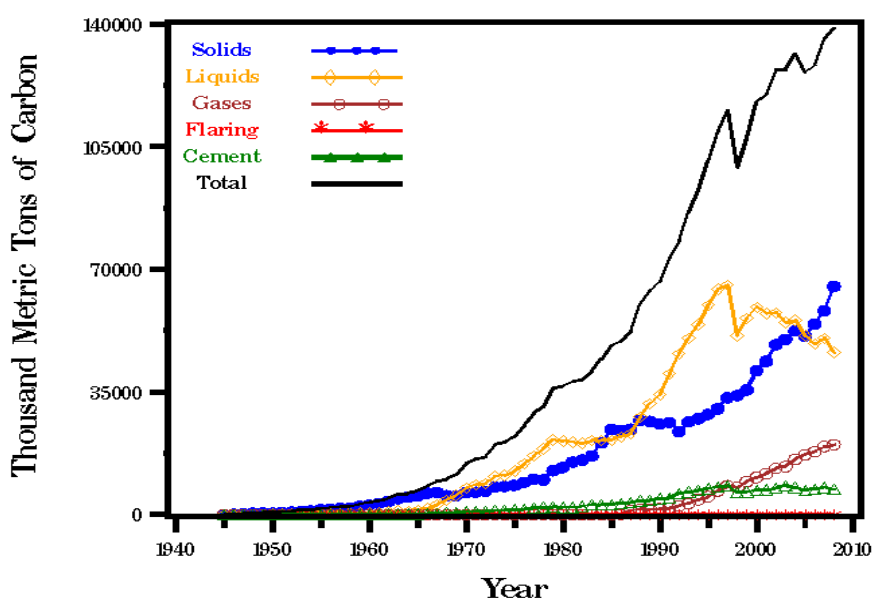
Figure.2: The CO_2 Emission trend, Republic of Korea.

On January 1, 2015, South Korea launched an emissions trading system that covers roughly two-thirds of the country's emissions. Emissions trading is a key policy toward meeting South Korea's target of reducing greenhouse gas emissions 30 percent below business as usual levels by 2020. Therefore, the South Korean carbon market is the world's second-largest, behind the European Union Emissions Trading Scheme [7]. It is also the second nationwide emissions trading program in Asia, following the launch of Kazakhstan's ETS in 2013.

Despite the challenges, Korea has set a target by 2030, which is expected to be in line with the recommendations of the IPCC Fifth Assessment Report to reduce global greenhouse gas emissions by

5

40-70% from 2010 levels by 2050. In order to achieve the objective of the United Nations Framework Convention on Climate Change of holding the increase in the global average temperature below 2℃ above pre-industrial levels, Korea also aims to reduce its greenhouse gas emissions in a manner consistent with the recommendations of the IPCC Fifth Assessment Report [Republic of Korea first NDC-8].
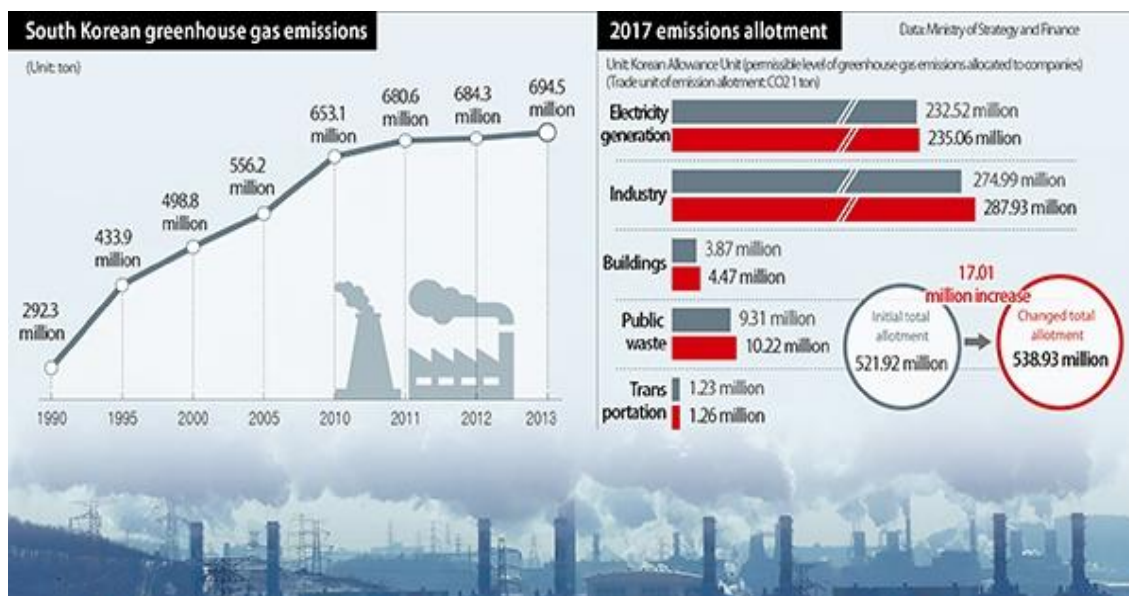
Figure.3: South Korean greenhouse gas emissions (Unit: ton) and 2017 emissions allotment (Trade unit of emissions allotment: CO_2 1 ton).

Several methods have been used for dry reforming process such as-thermal, catalytic, plasma activation and plasma catalytic over the last decade. Among all of them, plasma catalytic process is the best process to avoid the excess amount of carbon deposition and higher selectivity of desired products. In contrast, dry reforming is more demandable compared to steam reforming because of the reduction of greenhouse gas emissions and economically feasible process which uses carbon-di-oxide as a reactant feed gas instead of water.

Among all of light hydrocarbons, propane is the leading candidate among all natural gases as an alternative source for syngas production due to easily transportable and stored as a compressible liquid, and it can exist as a gaseous form at standard temperature and pressure. In case of reforming process, transition metals (Fe, Co, Ni and Cu) and noble metals (Ru, Rh, Pd, Ir and Pt) have given the most promising catalytic activity, especially in the reduced form [9]. In general, noble metals show

best catalytic activity towards dry reforming of methane, but the relatively high cost and unavailability in the nature of noble metals limits their utilization in the dry reforming process (DRP). In the DRP process, Ni-based catalyst has been widely tested and exhibited a promising catalytic performance owing to its availability in nature, excellent activity and cost effective compared to noble metals. In this systematic research study, CeO_2 was used as a promoter which is highly oxidative basic rare-earth metals that are able to store and release lattice oxygen species, and it can react with deposits carbon. So it is capable of repel coke formation due to quickly re-oxidize reactions of forming a Ni-CeO_2 nanocomposite and enhancing the catalytic activity and long term stability. On the other hand, the selection of suitable acidic/basic support material is the most important factor for dry reforming which is influencing the carbon deposition. Carbon deposition is formed easily on acidic supports such as SiO_2 while different researchers have reported that Lewis base supports such as Al_2O_3 reduce carbon deposition [10]. Lewis bases have a high affinity for the chemisorptions of CO_2 and it has been suggested that adsorbed CO_2 reacts with deposits carbon to form CO, thereby reducing coke formation [11]. The support which is used in the DRP process should maximize the surface area, provide a high dispersion of the active metal and be stable at high temperatures. However, $ɤ/Al_2O_3$ is more suitable support material to hold the metal oxides in the dry reforming process according to numerous observations.

2.2 Propane

Propane is a three-carbon alkene with the molecular formula C_3H_8 which is a by-product of natural gas processing and petroleum refining process. Generally, it is used as a fuel and very easy to compressible to a transportable liquid petroleum gas (LPG). The CAS number of propane is 74-98-6. The below figure 2.4 shows the internal structure of propane.
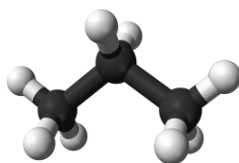
Figure.4: Atomic structure of Propane (Wikipedia).

2.2.1 Physical Properties

C_3H_8 is a gas at standard temperature and pressure. It is odorless, colorless, tasteless and flammable gas, which is light hydrocarbon. The boiling point of C_3H_8 is 230.90 to 231.11 K and its molar mass is 44.10 g·mol^{-1}. The solubility in water is 47 mg L^{-1} and it is used as a feedstock for the production of base petrochemicals in steam cracking and also inexpensive, high-energy fuel for explosions and other special effects.

2.2.2 Chemical Properties

Table. 1. Presents the lists of chemical properties of C_3H_8 at 298k.

Chemical properties	Value
Standard enthalpy of formation, $\Delta H^0_{298\,k}$	−104.7 kJ/mol
Standard enthalpy of combustion, , $\Delta H^0_{298\,k}$	−2202.0 kJ/mol
Standard molar entropy, $S^0_{298\,k}$	269.91 J/k mol
Specific heat capacity, C_p	73.60 J/k mol

2.3 Carbon Dioxide

Carbon dioxide is the most significant long-lived unwanted material which is responsible for greenhouse gas in the earth's atmosphere. In particular, CO_2 is produced by the combustion of wood and other organic materials, fossil fuels such as coal, peat petroleum and natural gas etc. as a waste of by-product. Human activities are also a major source of CO_2 and the global average concentration of CO_2 in Earth's atmosphere is currently about 0.04%, or 400 parts per million by volume (ppm) [12].
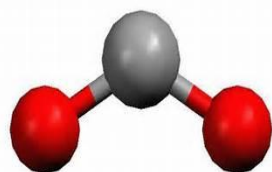
Figure.5: Atomic structure of CO_2 (Wikipedia).

2.3.1 Physical Properties

- ❖ Carbon dioxide is a colorless odorless gas, which is soluble in water, ethanol, and acetone.

- ❖ Melting Point : -55.6^0C

- ❖ Boiling Point : -78.5^0C

- ❖ Density : 1.977 kg/m^3

- ❖ Molecular Weight (lb/mol): 44.01

2.3.2 Chemical Properties

- ❖ Carbon dioxide is a linear covalent molecule.

- ❖ Carbon dioxide is an acidic oxide and reacts with water to give carbonic acid.

- ❖ Carbon dioxide reacts with alkalis to give carbonates and bicarbonates.

- ❖ CO_2 is not reactive with water.

- ❖ CO_2 is a non-toxic compound at $-78.9°C$ temperature and releases 645 KJ/Kg energy when heated from $-78.9°C$ to $0.0°C$ (Aresta and Forti, 1986-13).

2.4 Industrial Application of Syngas

Synthesis gas (syngas), is a mixture of hydrogen and carbon monoxide with different ratios. The sources of syngas are ubiquitous in nature, which is manufactured from natural gas, coal, petroleum, and biomass and even from organic wastes. The use of synthesis gas (syngas) in industry can easily produce a broad range of environmentally clean fuels and chemicals. Almost maximum amount of hydrogen gas is produced from syngas in different ways and there has been a tremendous spurt in the demand for this widely used gas; indeed, the chief use of syngas is in the manufacture of hydrogen for a growing number of purposes [14]. The present and future uses of syngas and its separate components (hydrogen and carbon monoxide) are the key topic to date with the availability and flexibility of the resource. Syngas is a major source of environmentally clean fuels and chemicals in

this modern world, and it could potentially use to produce pollution-free electricity, which can remove sulfur and nitrogen at a large extent from air. Syngas generation process is depicted as a syngas cycle in Figure 6 (15-Rostrup-Nielsen, 2002).
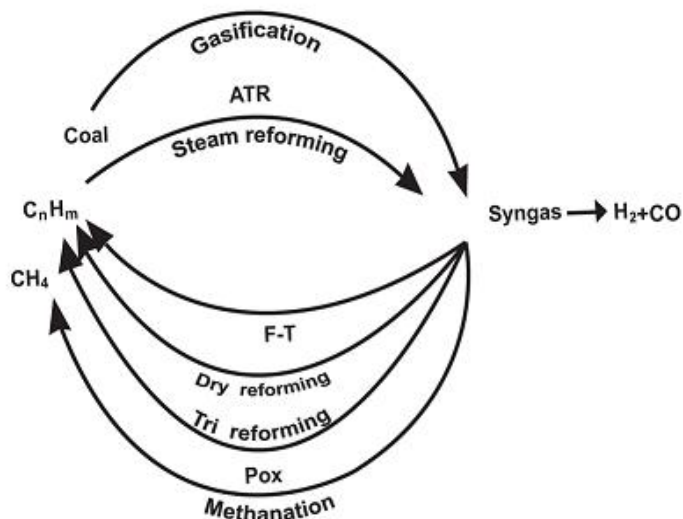
Figure.6: The Syngas Cycle

So, Syngas is the major source building block for liquid fuel production via Fischer-Tropsch (F-T) process and also in the chemical and petrochemical industries such as methanol and ammonia production [12].

Reforming of natural gas represents the lowest cost route to production of syngas [17], which has found a wide range of uses in synthetic chemical industries as shown in Figure 7.
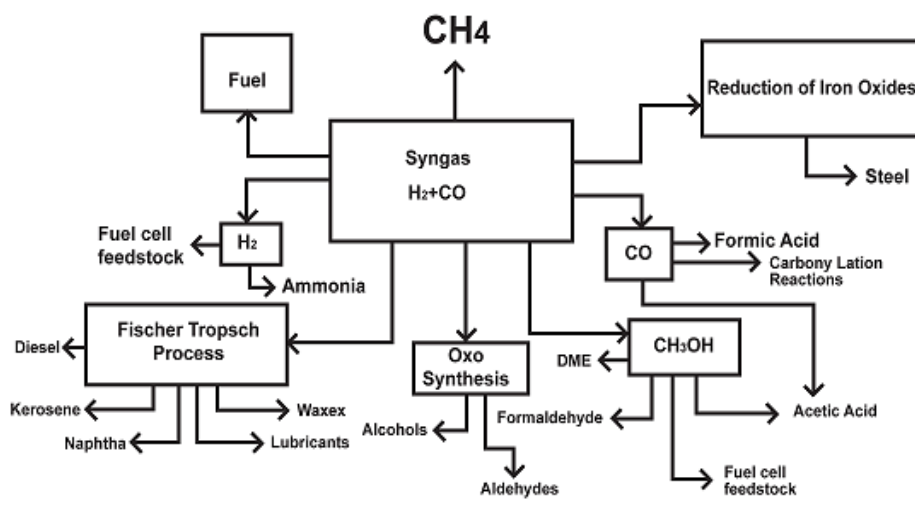
Figure.7: Schematic diagram showing the main applications of syngas.

10

2.5 Types OF Reforming Technology

This section will discuss about different types of industrial approaches in reforming technology for syngas generation which is determined by the desired level of H_2/CO ratio and the plant requirements.

2.5.1 Steam Reforming

Steam reforming is an advanced, highly endothermic reaction process which is carried out between natural gas or other light hydrocarbons and steam in the range of 1000-1273°C over heterogeneous catalysts with a H_2/CO ratio of three (Gaur, 2011) [18]. This technology requires higher operating pressure (30-40 bars) compared to dry reforming and it increases the operating cost. Normally, SMR refers to methane (CH_4) reacts with steam (H_2O) in the presence of Ni-based catalysts generate syngas and CO_2. The steam reforming hydrocarbon of is produces around 95% of hydrogen for refining process (Guido and Foster *et.al.* 2011) [19]. SMR is an industrially recognized process that can produce higher hydrogen selectively and it involves two most important reactions at high temperature and another is one at low temperature such as:

$$CH_4 + H_2O \rightarrow CO + 3H_2 \qquad \Delta H° = 241 \text{ kJ mol}^{-1} \qquad (1)$$

$$CO + H_2O \leftrightarrow CO_2 + H_2 \qquad \Delta H° = -41 \text{ kJ mol}^{-1} \qquad (2)$$
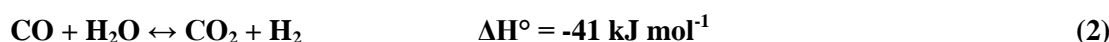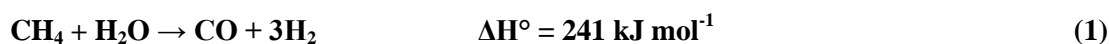
Hence, steam methane reforming is the first choice for industrial applications because it produces a relatively higher hydrogen-to-carbon ratio.

Limitations:

- High operating cost.

- Catalyst deactivation and sintering is the main problem in reforming due to excess amount of carbon deposition.

- High steam partial pressure and high mass velocity (large Reynolds number) resulting in rapid deactivation.

- Huge amount of water is needed to conduct steam reforming as a raw material.

11

2.5.2 Dry Reforming Technologies

Dry reforming is an advanced breakthrough technology for syngas production, although it's now under development process. DRM is the reaction of CH_4 with greenhouse gas (CO_2) to produce syngas with a H_2/CO ratio of two which is more suitable for liquid-fuel synthesis (18). Dry reforming is an endothermic reaction mechanism and it has great significance in industrial applications due to the desirable consumption of CO_2 as a GHG.

According to Rostrup-Nielsen et al., replacing the steam with carbon dioxide has real impact on the chemical reaction mechanism meaning the kinetics of steam reforming is very close to that of dry reforming [15]. Actually DRM is principally an endothermic reaction that needs an operating temperature of 900–1273 °C and pressure close to 1 bar in order to attain high equilibrium conversion of reactants (CH_4 and CO_2) to products (H_2 and CO). Since it has low (H_2/CO) ratio, it undergoes complete conversion. Due to abundance of CO_2 in atmosphere, dry reforming is more suitable process in remote gas fields instead of water. According to Fidalgo and Menendez (2011), the decomposition of CH_4 is the main cause for carbon formation at higher temperature. In fact, Dry reforming process is also suffering with catalyst deactivation due to carbon deposition on the surface of support material [20]. To reduce carbon formation on support material, DRP of CH_4 is usually conducted at temperatures > 750 °C, where carbon formation is less favorable thermodynamically [21]. Furthermore, the severity of carbon deposition is more pronounced in dry reforming of methane than for SMR or partial oxidation of methane due to the low O/C atomic ratio in the feed gas, which can get worse with higher CO_2 content [22]. However, the DRM main reaction (Eq. 3) is followed by three side reactions (table 2): (i) methane decomposition (Eq. 4), (ii) Boudouard reaction (Eq. 5) and (iii) Revers water gas shift (RWGS) reaction (Eq. 6). The carbon deposition minimization analysis through thermodynamics and chemical reaction mechanisms generally use the Gibbs free energy methods [20-22] which demonstrates that the first two factors are responsible for the catalyst deactivation due to carbon deposition. On the contrary, Methane decomposition (Eq. 4) is favored at low temperature thermodynamically while high temperature usually favors the Boudouard reaction (Eq. 5).

Table 2: The DRM reactions.

Reaction Mechanism	Reaction	ΔH° 298K kJ·mol-1	Reaction Priority	Eq.
DRM	$CH_4 + CO_2 \leftrightarrow 2CO + 2H_2$	247	Main Reaction	3
Methane Decomposition (Methane Cracking)	$CH_4 \leftrightarrow C + 2H_2$	75	Side reaction	4
Boudouard (CO Disproportionate)	$2CO \leftrightarrow CO_2 + C$	-171	Side reaction	5
Revers Water Gas Shift (RWGS)	$CO_2 + H_2 \leftrightarrow CO + H_2O$	41	Side reaction	6

So, dry reforming of methane with CO_2 is an attractive process to reduce the destructive greenhouse gases from an environmental perspective and economically very feasible in real time industrial applications. Currently, the Calcor process and the SPARG (sulfur-passivated reforming) process are two major advanced methods for minimizing the problem of carbon formation in dry reforming technology [5].

Limitations:

- Thermodynamically, catalyst deactivation is the major disadvantage due to coke formation during the dry reforming reaction.
- Dry reforming reaction occurs at high temperature.
- Carbon deposition is more compared to SMR.

2.5.3 Tri Reforming

Tri-reforming concept is a new advanced technology for syngas production, which was first developed by Song in 1999 using power plant flue gas. Tri-reforming is an effective process to consume greenhouse gases like methane and CO_2 to produce syngas with a higher H_2/CO ratio for FTS. Tri reforming is mainly designed for the direct synthesis gas production with expected H_2/CO ratios by methane or natural gas reforming using flue gas of fossil fuel based electric power plants

13

without pre-separation of CO_2. In general, flue gases of natural gas-fired power plants typically consist of 8-10% CO_2, 18-20% H_2O, 2-3% O_2, and 67-72% N_2; flue gases from coal-fired boilers mainly consists of 12-14% CO_2, 8-10% H_2O, 3-5% O_2, 72-77% N_2, and trace amount of NOx, SOx, and particulates [24]. Other features of tri-reforming is that there is no need to handle pure oxygen and it can directly produce synthesis gas with a proper H_2/CO ratio (e.g. $H_2/CO = 1.5 \sim 2$). In general, the new concept of tri-reforming technique is very consistent with the set goals of DOE Vision 21 for power plants with respect to the decrease of greenhouse gas emission with improvement of power generation efficiency and co-producing fuels and chemicals [25]. In reality, tri-reforming reaction, steam, CO_2, and O_2 all compete with each other to react with methane over catalysts, and the improvement of CO_2 conversion with the presence of steam and O_2 mostly depends on the catalysts and reaction conditions [26]. According to Song, the Catalytic tri-reforming of methane was achieved successfully with high CH_4 conversion (≥97%) and high CO_2 conversion (around 80%) for producing syngas with desired H_2/CO ratios of 1.5–2.0 over supported Ni catalysts at 1130-1273 °K and 1 bar without carbon formation on the catalyst. The most important promising factor is that it can dramatically inhibit carbon formation on reforming catalyst by oxidizing the coke to increase catalyst life and process efficiency [27].

The tri-reforming properties in an equilibrium condition under various conditions were examined by thermodynamics, while CO_2 gives a higher equilibrium conversion than steam when same amounts of steam and CO_2 co-exist in Tri reforming. A tailored catalyst for tri-reforming is needed to attain higher CO_2 conversions in catalytic tri-reforming of methane. According to the aforementioned established concept, the flue gas (CO_2, H_2O, and O_2) obtained from fossil-fuel-based power plants can be used as co-reactants for tri-reforming of methane to produce syngas [26]. The schematic diagram of tri reforming process is shown in figure 8.
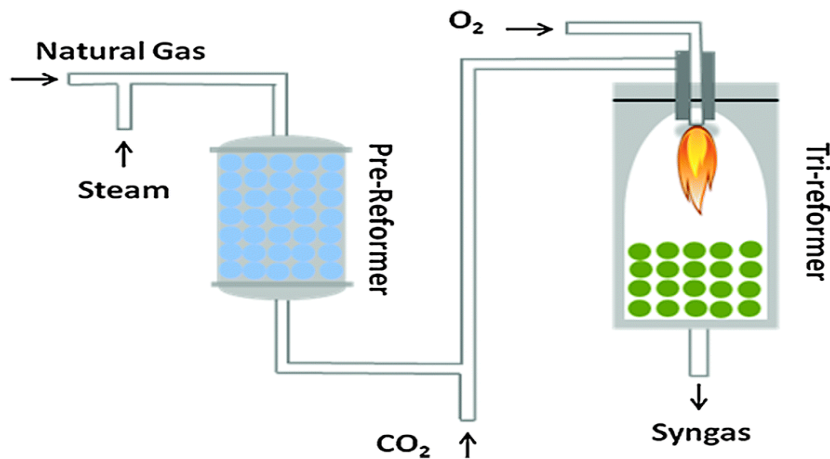
Figure.8: General concept for tri-reforming using flue gas from fossil fuel-based power plants

(Wikipedia).

2.5.4 Auto-thermal Reforming

Auto-thermal reforming is an exothermic reaction mechanism which was first proposed by Haldor Topsøe in 1950 and industrially recognized technology for desired syngas production. ATRM combines the both steam methane reforming and partial oxidation of methane reforming in a single reactor which is evaluated at high temperature around 1573 °K . Among all other reforming techniques [26], the ATR has been considered a promising technique due to its high efficiency, simplicity, more controllable H_2/CO ratio and user friendly process start-up [28]. The auto-thermal reactor is designed in two parts (an upper combustion zone and a lower catalyst bed zone) for best performance as shown in Figure 9.

$$CH_4 + x\ H_2O + (1 - x/2)\ O_2 \rightarrow CO_2 + (x + 2)\ H_2 \tag{7}$$
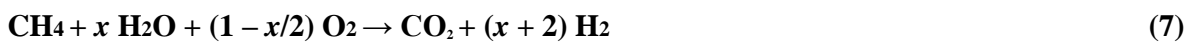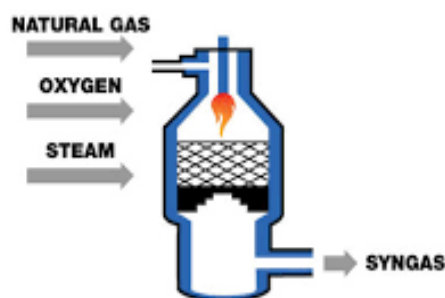
Figure.9: Diagram of an ATR reactor (Wikipedia).

As a result, Auto-thermal reforming process represents a flexible choice and providing a reasonable H_2 and CO yields in a moderate cost with more responsive compared to SMR.

Limitations:

- The hot stream accelerates the thermal sintering and deactivate the supported catalyst.

- It requires extensive control system to ensure proper robust operation.

2.5.5 Partial Oxidation Using Oxygen (POX)

Partial oxidation of methane is a considerably exothermic reaction process which is easily undergoes with or without the presence of catalysts with very less CO_2 content. Gaur et.al. (2011) reported that POX process produces syngas with a H_2/CO ratio of two, which is more suitable for F-T synthesis [12]. In non-catalytic POX, methane is mixed with excess O_2 and ignited. Temperatures of > 1127 °C and pressures of $50 - 70$ atm are needed to conduct the large scale conversions of methane in POM process. Different types of transition and noble metal supported catalysts have been utilized for POX reforming process. However, the high running costs of this process have made it uncompetitive with SMR. The main setbacks are due to the costs of separating the O_2 reactant from air and the need for a soot scrubber system downstream of the reformer, as well as the problems of high energy input, catalyst deactivation and sintering that also plague the SMR process.

$$CH_4 + \frac{1}{2} O_2 \rightarrow CO + 2H_2 \qquad \Delta H° = -36 \text{ kJ mol}^{-1} \qquad (8)$$
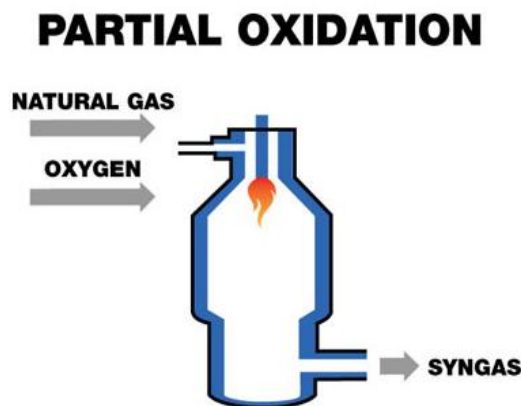
Figure.10: Diagram of POX reactor (Wikipedia).

16

Limitations:

- High pressure and pure oxygen are needed to conduct for POX process.

- More advanced studies and economic evaluations are required to develop this process for real time industrial applications.

2.5.6 Thermo-catalytic Decomposition of Methane

Generally, methane decomposition is considered as a high methane conversion process which is producing a CO_x free pure hydrogen for oil refineries, PEM fuel cells, and methanol and ammonia generation to avoiding product separation cost [29]. This process can regenerate the carbon based catalysts very effectively and to provide a stable life of catalyst over several cycles. Ni based catalysts are more suitable for methane decomposition and depending on the various operating conditions, the carbon formation is different such as filaments, carbon nanotubes, amorphous and graphitic forms.

$$CH_4 \rightarrow C\ (s) + 2H_2 \qquad\qquad \Delta H° = 76\ mol^{-1} \qquad\qquad (9)$$

So, this alternative process is the direct decomposition of methane to produce H_2 and solid carbon which is very easy to isolate from gaseous products [5].

Limitations:

- Catalysts are prone to sintering and deactivation at high temperatures and the methane conversion rates are thermodynamically limited at lower temperatures.
- Non-catalytic methane decomposition occurs at higher temperature > 1200°C.

2.6 Thermo-dynamical Study

Thermodynamic analysis is the fundamental study about reforming process development which can be fruitful in chemical reaction engineering. Generally, it provides a suitable strategy about the product distribution with the combined effect of process parameters and find the optimum conditions to maximize the desired products for certain important industrial applications. Such studies are very important to start experimental programs for catalyst and process development.

Over a period of decades, the thermodynamic study was conducted with the development of a mathematical model of the process using ChemCAD process simulator a well-known and widely used CAPE tool [30]. Numerous thermodynamic studies have been published for different processes such as steam reforming of ethanol, sorption enhanced steam reforming of butanol and propane, oxidative steam reforming of propane, glycerol steam reforming with in-situ hydrogen separation, steam reforming of dimethyl ether, dry autothermal reforming of glycerol , and so forth [31]. In contrast, these studies have been limited to hydrogen or syngas production only without any comprehensive research study on optimum thermodynamic conditions to maximize the desired combined products and minimize the undesired products.

However, DRM studies have shown that the thermodynamic equilibrium fundamentals are interconnected to the kinetic mechanisms and it plays a vital role for efficient process control, both from energy/cost considerations and catalyst deactivation inhibition methods. In general, it can be predicted that the thermodynamics determine "if reaction will occur" and kinetics determine "how it will occur".

 It can be concluded that thermodynamic variables including temperature, pressure and reactant ratio have a wide range of significant effects on the reaction rate, products distribution and by-product formation, respectively [32].

2.7. Overview of Plasma Technology

2.7.1. Plasma

A Plasma is quasi-neutral gas of charged and neutral particles which exhibits collective behavior [33]. In other words, Plasma is a gas in which a certain portion of the particles are ionized that contains a large number of different species existing in plasma including positive and negative ions, free radicals, electrons, molecules and gas atom in the ground or any higher state of any form of excited species [34].

18
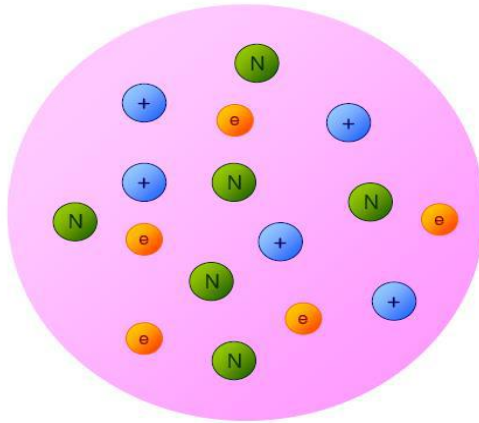
Figure.11. Internal existence of plasma

In practical, Plasma is a fourth-state matter distinct from solid or liquid or gas and present in stars and fusion reactor; a gas becomes a plasma when it is heated until the atoms lose all their electrons, leaving a highly electrified collection of nuclei and free electrons [35].
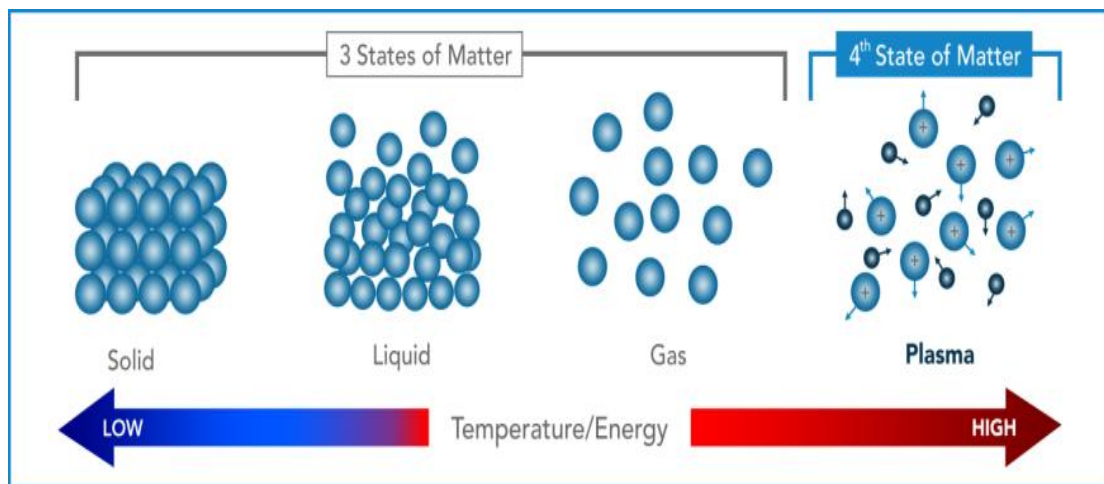
Figure. 12: Basic of Plasma generation.

After all, the collision between charged and neutral particles leads to an ionization which is a very crucial issue to sustain the plasma smoothly.

2.7.2 Classification of Plasma

Several methods including electrical discharges such as corona, glow, arc, microwave discharge, plasma jets, radio frequency (RF) and DBD have been applied for the generation of plasmas in catalyst preparation and other activities [5]. Usually, plasmas are generated by applying direct and

19

alternative high (AC) voltage to a gas or a gas mixture in the laboratory and industrial applications. In general, plasmas are classified into two main types such as high and low-temperature plasmas (including thermal and non-thermal plasma) depending on the temperature and energy levels which is shown in table 3.0. In addition, when the kinetic temperature of the electrons in the gas (plasma) is equal to the temperature of the heavy species (atoms, ions, molecules), then the plasma is called as thermal plasma.

Table. 3. The DRM reactions.

Low Temperature Plasma (< ~eV)		High Temperature Plasma (10 > keV)
Non-Thermal Plasma	Thermal Plasma	
1. Consisting of neutrals, electrons, and ions (abundant neutrals and **radicals**). 2. Industrial plasmas.		1. Consisting of electrons and ions (charged particles). 2. Nuclear fusion plasma.
$T_0 \approx T_i \approx T_r < T_v \ll T_e \leq 105\ K$	$T_0 \approx T_i \approx T_r \approx T_v \approx T_e \leq 2 \times 104\ K$	$T_0 \approx T_i \approx T_r \approx T_v \approx T_e \geq 107\ K$
1. Corona discharge 2. DBD 3. Microwave discharge 4. Plasma jet (atmospheric pressure)	1. Microwave discharge 2. Glow discharge 3. Gliding arc discharge (atmospheric pressure)	

2.7.3 Generation of Non-Thermal Plasma by Electric Fields

To date, the applications of non-thermal plasma (NTP) generated by electrical discharge under ambient atmosphere have been attracted a great research interest in academic and industrial sectors.

20

The non-thermal plasma is usually formed by the application of an external electric field between two electrodes surrounded by a volume of gas and it can be operated at low pressure (1 – 103 Pa), atmospheric pressure and above.

However, the breakdown voltage (V_b) is the minimum voltage required to breakdown a gas to form a plasma discharge and the V_b is mostly dependent on the reactor gas pressure (p) and the distance between two electrodes (d) according to the geometry of reactor. The relationship among gas pressure, electrode gap distance and V_b is described by Paschen's Law (10), where a and b are constants that are dependent on the gas type [5].

$$V_b = \frac{a(pd)}{ln(pd)+b}$$ .... (10)

When the breakdown voltage is reached at a certain point depending on plasma parameters, the current flow increases sharply due to the avalanche electrons in the discharge gap between the two electrodes. These high energy electrons usually collide with gas molecules leading to the formation of new 'active' plasma species, including excited molecules and atoms, and their relevant degrees of freedom, radicals, ions and new stable gas molecules. These collision processes are shown in Table [5].

Table. 4. Collision processes.

Electron/Molecular Reactions	
Excitation	$e\text{-} + A2 \rightarrow A2^* + e\text{-}$
Dissociation	$e\text{-} + A2 \rightarrow 2\,A + e\text{-}$
Attachment	$e\text{-} + A2 \rightarrow A2\text{-}$
Dissociative attachment	$e\text{-} + A2 \rightarrow A\text{-} + A$
Ionisation	$e\text{-} + A2 \rightarrow A2\text{+} + 2\,e\text{-}$
Dissociative ionisation	$e\text{-} + A2 \rightarrow A\text{+} + A + e\text{-}$
Recombination	$e\text{-} + A2\text{+} \rightarrow A2$
Detachment	$e\text{-} + A2\text{-} \rightarrow A2 + 2\,e\text{-}$
Electron/Molecular Reactions	
Penning dissociation	$M + A2 \rightarrow 2\,A + M$
Penning ionisation	$M^* + A2 \rightarrow A2\text{+} + M + e\text{-}$
Charge transfer	$A\pm + B \rightarrow B\pm + A$
Ion recombination	$A\text{-} + B\text{+} \rightarrow AB$
Neutral recombination	$A + B + M \rightarrow AB + M$

Decomposition		Synthesis	
Electronic Atomic	e- + AB → A + B + e-	Electronic	e- + A → A* + e-, A* + B → AB
Atomic	A* + B2 → AB + B	Atomic	A + B → AB

A small portion of the energy is transferred to the new active plasma species during collisions between electrons and heavy gas molecules due to the relative sizes of the species involved. The gas is weakly ionized for certain amount in most of the non-thermal plasma systems. The degree of ionization in the plasma is the ratio of the density of charged particles to the density of neutral species and the range is $10^{-7} - 10^{-14}$ [9].

So, NTP (non-thermal plasma) approach is energetically feasible and it has some specific advantages such as easy operating conditions mainly consists of electrons, excited atoms and molecules, meta stable ions, radicals, neutral particles and so on. More precisely, these highly energetic electrons initiate the chemical reactions in the gaseous phase and most of the energy will be used for accelerating electrons due to low degree ionization (22-23). Thus, non-thermal plasma is a very promising technique for catalyst modification/reduction, improved dispersion, better anti-carbon deposition and better low-temperature activity, enhanced stability and extensively improve the catalyst performance.

In the last decade, several plasma techniques were used to convert CO_2 and CH_4 into syngas such as thermal plasma (TP), dielectric barrier discharge (DBD), corona discharge (CD), AC arc discharge (AD) and glow discharge (GD) [9]. Although Plasma techniques have demonstrated a fast conversion and easy realization, but its conversion efficiency still needs to be improved for future industrial applications and researchers are trying to combine catalyst and plasma in CO_2 and CH_4 reforming system nowadays [36]. The widely used DC Plasma discharge technology and their typical reactor configurations are discussed in the following sections briefly.

2.7.3.1 Corona Discharges

Corona discharge is an electrically discharged process by which a current flow from an electrode with a high potential into a neutral fluid, usually air, by ionizing that fluid so as to create a region of plasma around the electrode that is electrically charged. In general, corona discharge usually occurs at highly curved regions on electrodes, such as sharp corners, projecting points, edges of metal surfaces, or small diameter wires, and the high curvature causes a high potential gradient at these locations so that the air breaks down and creates plasma there first. Coronas can be positive or negative type, but the type is defined by the polarity of the voltage on the highly curved electrode. Thus, the corona is called positive corona if the curved electrode is positive with respect to the flat electrode.
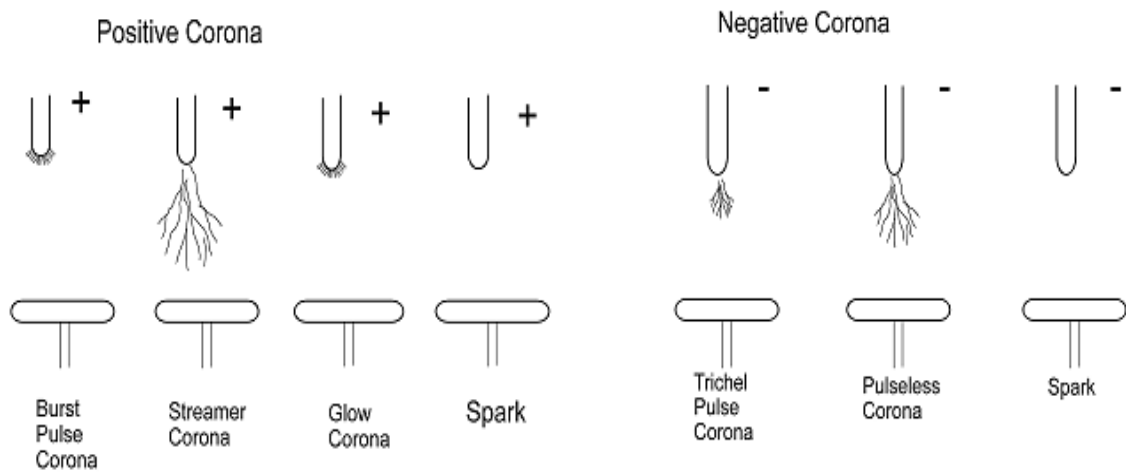
Figure.13: Schematic diagrams showing different forms of corona discharges in a point-to-plate electrode configuration [9].

The corona discharge reactor is generally made of two electrodes, a top metal wire electrode and a lower hollow electrode as the grounded one. Corona plasma discharge can result in high conversions of methane and carbon dioxide compared to the result of non-plasma reactions. Moreover, the corona discharge takes place between the two electrodes occupied by a continuous flow of gas and occurs at atmospheric pressure and low temperature.
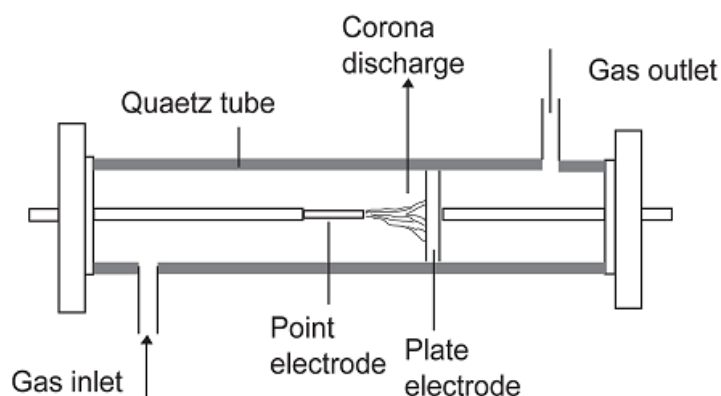
Figure.14: Schematic diagram of a corona discharge reactor in a point-to-plate configuration [5].

For a point-to-plate electrode configuration, the different types of corona discharge are shown in Figure 14, where the applied voltage increases from left to right. Positive corona is formed at a pointed anode, whilst negative corona is formed at a pointed cathode. In both positive and negative corona, high current flow will result in complete breakdown and the formation of a single spark discharge that bridges the discharge gap.

2.7.3.2 Glow Discharge

Glow discharge is a novel plasma reduction method that has been developed to reduce supported noble-metal ions without the use of any reducing chemicals and formed by the passage of electric current through a gas [37]. Glow discharge is a simple type of direct current glow discharge and it consists of two electrodes in a cell held at low pressure (0.1–10 Torr) which is used to increase the mean free path. For the electric field, a longer mean free path allows a charged particle to gain more energy before colliding with another particle [38]. Plasma process offers the best reaction mechanism to induce gas phase reaction, which is utilized in many chemical reactions for better output. Atmospheric pressure glow plasma discharge offers a high conversion ability due to its special plasma parameters (electron density, electron energies, plasma temperature lower than thermal plasma, higher

24

than non-thermal plasma such as DBD and corona discharge, feed gases (CO_2 and CH_4) served as direct discharge gas), which is several times higher than that of other discharge plasmas [39].

In analytical chemistry, glow discharges are usually operated in direct-current mode and may also be operated in radio-frequency and are used as a source of light in devices such as neon lights, fluorescent lamp, and plasma screen televisions.
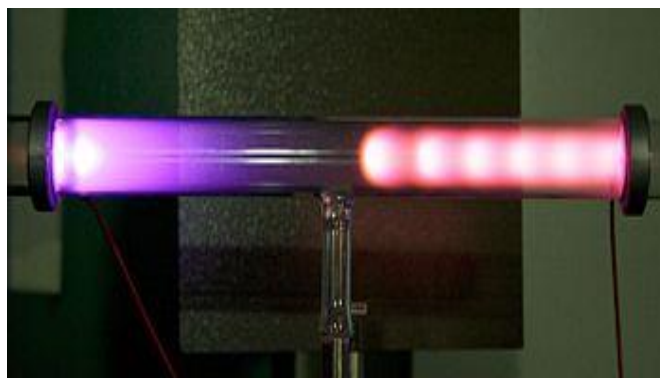
Figure.15: A Crookes tube illustrating the different glowing regions that make up a glow discharge [Wikipedia].

2.7.3.3 Gliding Arc Discharges

Gliding arc discharge plasma has received the major research interest over the last decade in different applications such as environmental applications, energy conversion, material processing and medical science. However, the energy utilization rate of a gliding arc discharge is very high because above 80% of the input electrical power is consumed for chemical reactions [40].

The gliding arc (GA) is a unique non-thermal plasma that has a relatively high plasma density, power and operating pressure in comparison with other non-equilibrium discharges. GA discharge reactor is consisted of two electrodes, one of which connected to the ground and the other connected to the high voltage power supply, and it can be operated at high atmospheric pressure [41].

The gliding arc (GA) is an intermediate system which generates regions of both thermal and non-thermal plasma at the conditions of atmospheric pressure and ambient temperature. It is able to

25

provide simultaneously high plasma density, power and operating pressure with high level of non-equilibrium, high electron temperature, low gas temperature and possibility of stimulation selective chemical processes without any quenching. Gliding arc is considered one of the most attractive of the advanced oxidation techniques because of low equipment and energy costs and its greater efficiency [41].

An atmospheric pressure gliding arc discharge can be formed between two flat knives-shaped electrodes with a gas flowing between them, as shown in Figure 16. The discharge is initially formed at the point where the discharge gap is narrowest and proceeds to "glide" up the electrodes, pushed by the flow of gas.
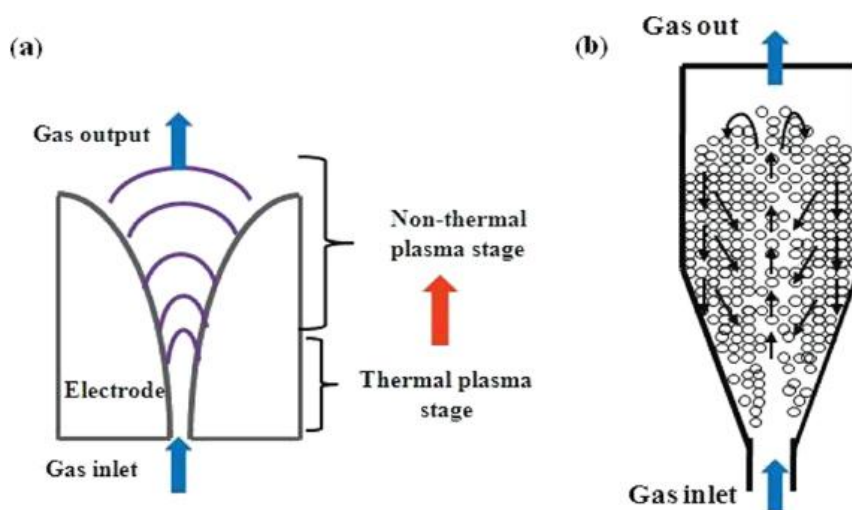
Figure.16: Schematic diagram of a gliding arc discharge reactor [Wikipedia].

So, gliding arcs may be thermal or non-thermal depending on the applied power and gas flow rates and these types of gliding arc plasma are potentially suitable in the chemical industry and environmental engineering.

2.7.3.4 Atmospheric Pressure Plasma Jet

The atmospheric pressure plasma jet (APPJ) or atmospheric pressure glow discharge is a well-established method of AC discharge that can initiate a non-thermal plasma regime at atmospheric

26

pressure. APAJ needs an inert gas such as helium or argon and it can generate stable, homogeneous plasma at atmospheric pressure, which can simultaneously provide a high electron temperature and a high energy density to achieve high selectivity and productivity in the reforming process. In addition, the special plasma jet designs make the feed gas pass through the discharge region, which is very convenient mechanism for the reforming reaction.

A high voltage inner electrode is surrounded by an outer electrode in the shape of a nozzle where the plasma is directed through the nozzle to form a plasma 'jet' shown in figure 17.
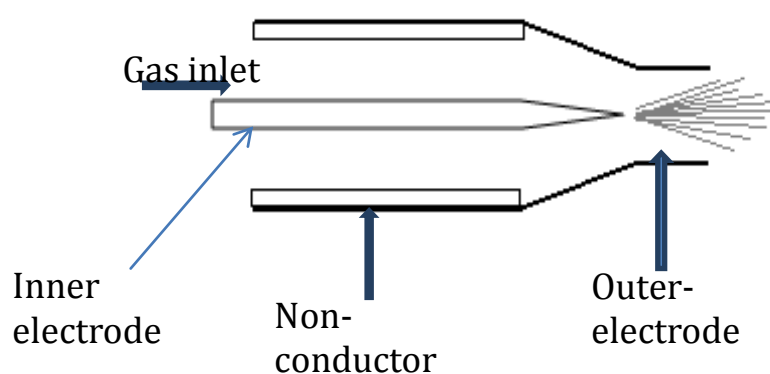
Figure.17: Schematic diagram of an atmospheric pressure plasma jet [42].

2.7.3.5 Radio Frequency Discharges

Radio frequency (RF) electromagnetic fields can be used to generate weakly ionized plasma at low pressures, typically in the range 1 – 103 Pa [42]. At higher pressures, the properties of the RF discharge will change as the collision frequency increases, leading to a discharge approaching a thermal regime when close to atmospheric pressure [43]. RF discharges usually operate at frequencies in the range 1 – 100 MHz corresponding to wavelengths in the range 300 – 3 m [42]. A RF discharges are particularly advantageous for applications that require the electrodes to be outside of the discharge region, thereby preventing contamination with metal vapors given off at the electrodes [43]. The two main types of RF discharge are capacitively coupled plasmas (CCPs) and inductively coupled plasma (ICPs); however, the frequency of 13.56 MHz (λ = 22 m) is particularly common for industrial applications.

On the other hand, a radio-frequency (RF) helicon plasma reaction chamber (HPRC) is developed and used to decompose methane gas into high-purity hydrogen gas and solid carbon in the form of graphite [5].

2.7.3.6 Microwave Discharges

Microwave discharges are widely used for generation of quasi-equilibrium and non-equilibrium plasma for different applications. Microwave discharges (MD) are the electrical discharges generated by the electromagnetic waves with frequencies exceeding 300 MHz [44]. Diagnostics of microwave plasma is complicated by presence of microwave field and non-uniformity of plasma.

2.7.3.7 Dielectric Barrier Discharges

Dielectric Barrier Discharges (DBD) was first reported by Ernst Werner Siemens in 1857, which is one of the best methods of non-thermal plasma treatment at atmospheric pressure and room temperature. In DBD, the electrical discharge takes place between two electrodes separated by an insulating dielectric barrier operated at atmospheric pressure [5]. This so-called dielectric barrier discharge is mainly responsible for a self-pulsing plasma operation and thus, the formation of a non-thermal plasma at normal pressure can occur. Furthermore, DBDs are also known as silent discharges, barrier discharges and ionizer discharges for naming. In general, dielectric materials such as glass, quartz, ceramics, enamel, mica, plastics, silicon rubber or teflon are used for DBDs in industrial applications.

DBD rector can be made in different configurations such as planar (using parallel plates separated by a dielectric) and cylindrical (using coaxial plates with a dielectric tube between them). The spacing in the discharge gap can vary from 0.1 mm to several centimeters depending on applications [5].
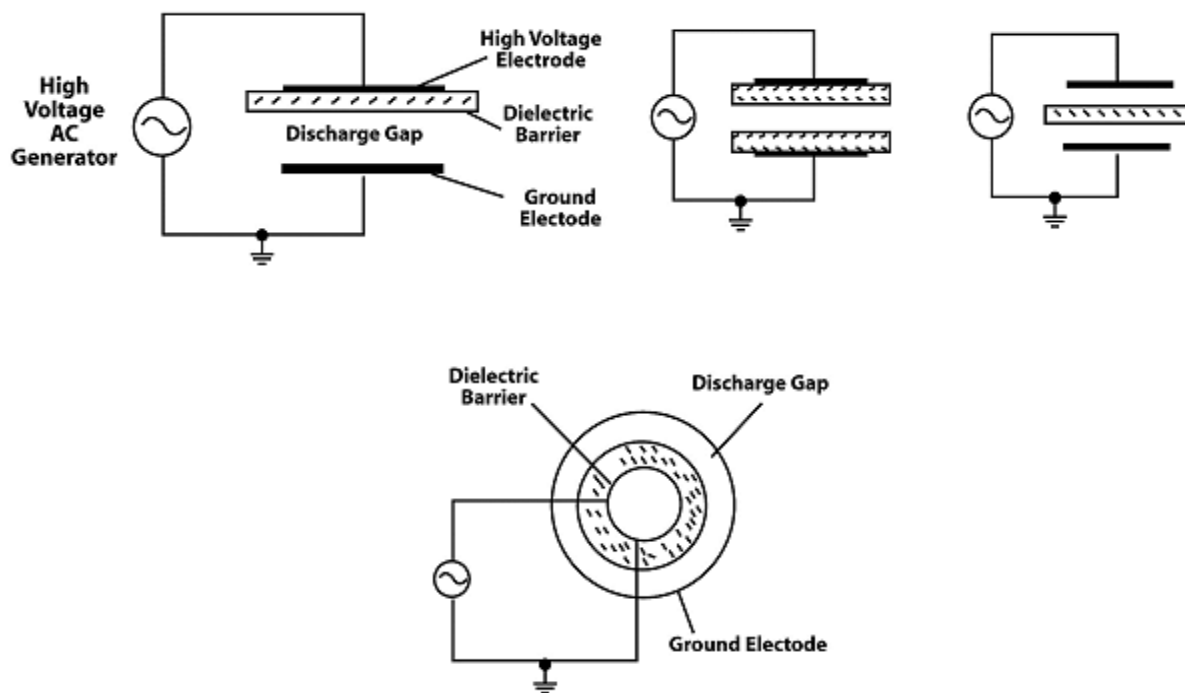
Figure.18: Basic dielectric barrier discharge configurations.

However, Dielectric barrier discharge (DBD) reactor is a hybrid plasma catalytic system which is widely used for syngas production via the carbon dioxide reforming of hydrocarbon. The DBDs techniques are truly beneficial to the further development of a plasma-based technique for the dry reforming of methane (DRM) with better output.

This experimental based research study was conducted with a coaxial dielectric barrier discharge (DBD) reactor for plasma-catalytic dry reforming of C_3H_8 into syngas over highly effective Ni-CeO_2/γ-Al_2O_3 catalysts. Moreover, gas molecules or radicals were adsorbed by catalysts to increase the probability of collisions between electrons and gas molecules during the DBD reactions for DRM process. As a consequence, the obtained results have revealed that the performance of the reaction is significantly improved with plasma-catalysis, which is much higher than the sum of plasma-alone and catalysis alone.

CHAPTER III

EXPERIMENTAL METHODS

This section describes in detail information about the used experimental techniques to characterize and investigate the entire dry reforming process; however, the analytical techniques used to measure the overall reaction performance as a function of variable experimental parameters have been explained.

3.1 Experimental Overview

The combination of non-thermal plasma and heterogeneous catalysts may give a synergistic effect to enhance the process performance in the plasma discharge zone with an appropriate DBD reactor configuration when syngas is produced from light (propane and ethane) hydrocarbon using a dry reforming process [3]. Plasma systems could address the aforementioned problems with optimum solutions in traditional reforming systems for better reactivity and efficiency. To do so, the plasma enhanced dry reforming system contains a significant number of chemically active species such as electrons, ions, atoms, radicals, and different wavelength photons which is more effective to increase catalytic activity and less carbon formation. Furthermore, the dielectric barrier discharge (DBD) is a non-thermal plasma phenomenon that can be operated at atmospheric pressure and driven by a sinusoidal AC voltage in the frequency range from 50 Hz to 500 kHz [5]. Therefore, DBDs can offer stable discharges in a range of different gases at relatively high discharge powers, making them particularly suitable for many industrial applications.

This investigation is basically focused on the non-thermal plasma catalyst treatment to initiate a new non-thermal plasma development for catalyst reduction, which can result in a better interaction between the metal and support materials during dry reforming reactions to prepare a more Ni active sites on the surface of support- γ/Al_2O_3. Therefore, it is essential to well disperse catalysts over the support material for increasing the desired reforming activity. The overall reaction of dry reforming of propane with CO_2 occurs through the following reaction:

$$C_3H_8 + 3CO_2 + 6Ar = 6CO + 4H_2 + 6\ Ar, \quad \Delta H^0_{298K} = 644.8\ KJ\ mol^{-1} \ ....(11)$$

In this investigation, very simple wet impregnation method was used to prepare Ni-CeO$_2$-γ/Al$_2$O$_3$ catalysts with 2 wt.% of Ni and 2 wt.% of Ceria contents which is a rapid and very simple approach for the preparation of catalysts. Dry reforming of propane was evaluated by operating the plasma in dielectric barrier discharge configuration and also conventional thermal process with Ni-CeO$_2$-γ/Al$_2$O$_3$ catalysts. Although dry reforming is an endothermic reaction that requires high temperature, but the purpose of the present study is to reduce the reaction temperature under the influence of plasma and develop a suitable catalyst using a plasma reduced process for higher syngas production rate possessed with high activity, stability, and minimum coking rate compared to thermally reduced process.

3.2 Catalyst preparation

Commercial γ/Al$_2$O$_3$ was used in this study as a catalysts support material (diameter: 3.2 mm, height: 3.7 mm and BET surface area: 179 m^2 g^{-1}) and it was purchased from Alfa Aesar Chemicals Ltd (Seoul, South Korea). The γ-Al$_2$O$_3$ support materials were impregnated with the aqueous Ni (NO$_3$)$_2$ 6H$_2$O and Ce (NO$_3$)$_2$ .6H$_2$O solution under 20 minutes vigorous stirring and finally, to obtain of the total 4 wt.% of Nickel and Ceria contents (2 wt.% each). After impregnation, it was dried in an oven at 110°C overnight to remove water before the calcination at 500°C for 5 h in air. So, the Ni-CeO$_2$-γ/Al$_2$O$_3$ catalyst contains 2 wt% of Ni and 2 wt% of Ceria. Subsequently, the prepared calcined Ni-CeO$_2$-γ/Al$_2$O$_3$ catalyst was put in a coaxial dielectric barrier discharge (DBD) reactor under Ar/H$_2$ (10%) atmosphere of total flow rate 100 ml min^{-1} at 500°C for 5 h. In the DBD reactor, the non-thermal plasma was generated using a cylindrical ceramic tube (inner diameter, outer diameter and thickness are 14.7, 20 and 2.7 mm, respectively) and a 3-mm concentric stainless-steel screw acting as the discharging electrode. In addition, the outer surface of the ceramic tube wrapped by a copper wire for 10 cm acts as the ground electrode via an external capacitor C$_{ext}$ (1μF). Initially, a certain amount

of the Ni-CeO$_2$-γ/Al$_2$O$_3$ catalyst pellets (12 g) was placed in between quartz wool plugs in the DBD reactor and powered by a high-voltage alternating current (AC) of 11.8-12 kV (operating frequency: 400 Hz) to generate non-thermal plasma in the catalyst bed. The voltage (V) and charge (Q) waveforms were recorded with a digital oscilloscope (TDS 3032, Tektronix) using an attenuation ratio of 1000:1 (P6015, Tektronix) as a high voltage probe, and the input power was measured by a digital power meter (WT200, Yokogawa). The voltage across the capacitor multiplied by its capacitance corresponds to charge accumulated in the reactor. The plasma input energy per cycle is equal to the area enclosed by the charge-voltage curve shown in the V-Q Lissajous charge-voltage figure (Figure 19).
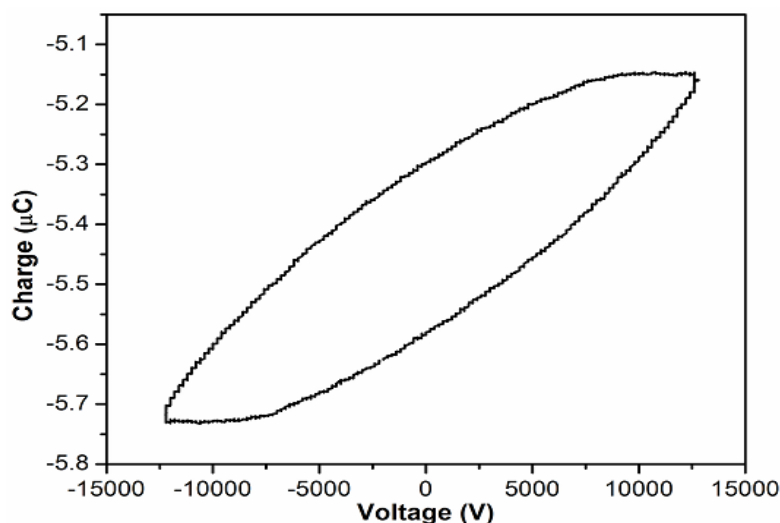
Figure.19: Calculated discharge power by the V–Q Lissajous method during catalyst preparation.

The specific input energy (SIE) was calculated by dividing the power with the flow rate of the gas.

$$SIE\ (J/L) = Power\ (J/s)\ /\ gas\ flow\ rate\ (ml\ min\text{-}1).$$

According to measurement, the discharge power was 2.1 J/s whereas the specific input energy was (SIE) =1260 J/L. In addition, the previously calcined fresh Ni-CeO$_2$-γ/Al$_2$O$_3$ catalyst was thermally reduced at 500°C under hydrogen atmosphere for 5 h to compare with plasma reduced catalyst for conversion efficiency.

32

3.3 Experimental Setup and Characterization of Reaction Performance
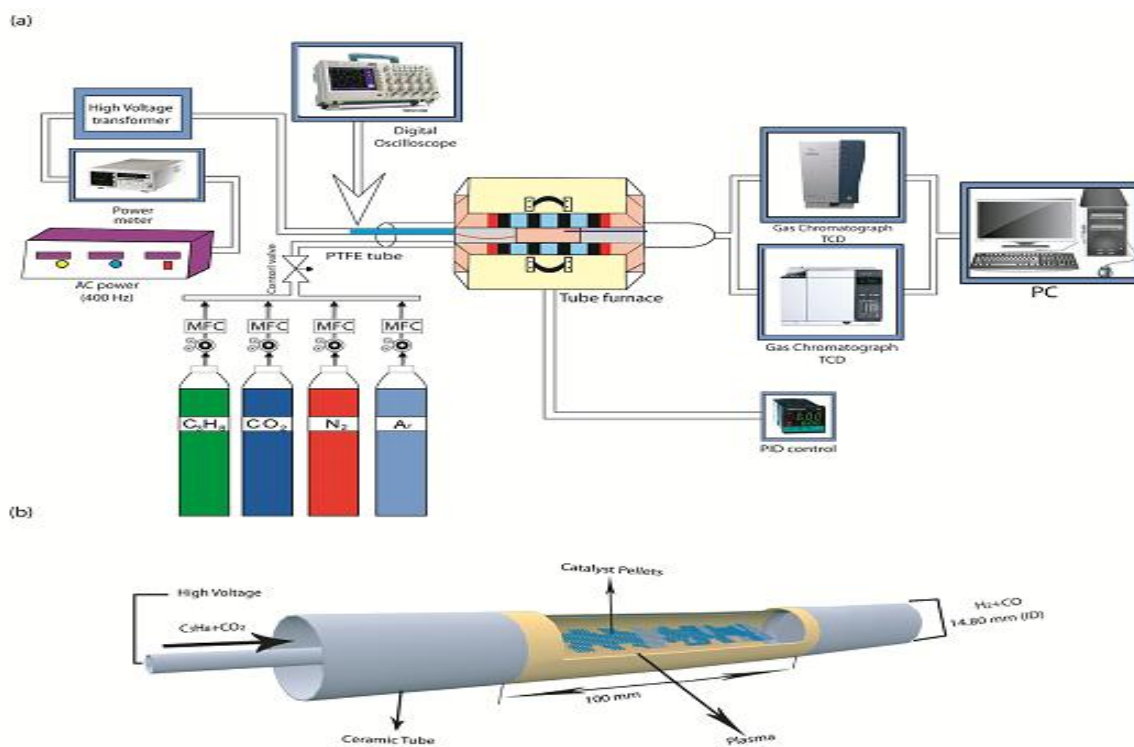
Figure.20: Schematic diagram of the experimental set-up used for plasma-assisted dry reforming of

Propane.

Figure. 20 (a & b) represents the total schematic diagram of the experimental setup for the dry reforming process. For better analysis, the catalytic evaluations were performed in both reactor such as thermo-catalytic reactor and DBD plasma catalytic reactor packed with 5 g of the catalysts pellets heated by an electric tube furnace. The reactor system was equipped with a set of mass flow controllers (MKS 1179A), which controlled the flow rate of each gas in the feed gas mixture. The reactant gases with a molar ratio of C_3H_8/CO_2 of 1/3 in balanced Ar (as a carrier gas) were fed into the reactor and the total gas flow rate was fixed at 300 ml min^{-1} under varied temperature range of 500-600°C for all of the catalysts in atmospheric pressure. Moreover, a thermocouple was inserted into the furnace chamber to measure the real time reactor temperature. During the dry reforming reactions, the concentrations of reactant gas components such as C_3H_8 and CO_2 were analyzed by a gas chromatograph (Micro GC CP-4900, Varian, 10 m Pora Plot Q column) and the analysis of product

33

gases (H_2, CO) were performed by DS-6200 GC equipped with thermal conductivity detector (TCD). Before starting the catalytic reaction, moisture, unwanted particles and gases were removed from the surface of the prepared catalyst by passing N_2 (flow rate of 200 ml min^{-1}) for 2 h at the reaction temperature.

To observe the direct plasma effect in reaction mechanism, DRP process was carried out with plasma or without plasma using both of the thermally reduced (TRC) and plasma reduced (PRC) catalysts at the temperature range 500 ~ 600^{0}C. When DRP process was conducted with plasma assisted reaction using plasma reduced catalysts, then it is called PRC + Plasma based DRP process. Similarly, TRC + plasma denotes when DRP process was performed with thermally reduced catalysts using plasma assisted reaction.

Table 5. Experimental parameter for the reforming reaction.

PRC + Plasma	PRC	TRC + Plasma	TRC
1. Temperature= 500-600°C	1. Temperature= 500-600°C	1. Temperature= 500-600°C	1. Temperature= 500-600°C
2. Catalyst load = 5gm	2. Catalyst load = 5gm	2. Catalyst load = 5gm	2. Catalyst load = 5gm
3. Carrier gas = Ar	3. Carrier gas = Ar	3. Carrier gas = Ar	3. Carrier gas = Ar
4. TFR= 300 ml min^{-1}	4. TFR= 300 ml min^{-1}	4. TFR= 300 ml min^{-1}	4. TFR= 300 ml min^{-1}
5. Reactant gas proportion = 10:30:60 ($C_3H_8/CO_2/Ar$)	5. Reactant gas proportion = 10:30:60 ($C_3H_8/CO_2/Ar$)	5. Reactant gas proportion = 10:30:60 ($C_3H_8/CO_2/Ar$)	5. Reactant gas proportion = 10:30:60 ($C_3H_8/CO_2/Ar$)
6. Applied Voltage = 10.3KV		6. Applied Voltage = 9.60 KV	
7. Discharge power = 2.6314 W		7. Discharge power = 2.2719 W	

34

To remove the solid coke formation on the prepared catalysts surface, the flow of reactant gas composition was stopped and set the reactor temperature to the desired value at 500°C. After stabilizing the desired temperature at 500°C, 200 ml min^{-1} of dry air was supplied inside the reactor, which could regenerate the deactivated catalysts by oxidizing the coke with an interaction of air [44].

The prepared catalysts were characterized by an X-ray diffractometer (Rigaku D/max-2200H) with a Cu Ka radiation source to analyze Powder X-ray diffraction (XRD) pattern. The presence of specific active elements and morphology were identified using a field emission scanning electron microscope (FE-SEM) coupled with an energy dispersive spectroscopy (EDS, JEM-1200EX II, JEOL) facility. Furthermore, a transmission electron microscope (TEM, JEM-2100HR, JEOL) and Raman spectroscopy were used to examine the surface structure and the particle distribution over the alumina support before and after reforming reactions. On the other hand, temperature programmed desorption (H_2-TPD and CO_2-TPD) and temperature programmed reduction (H_2-TPR) techniques were utilized to investigate the number of catalytic active sites and specific reduction of catalytic active sites depending on temperature.

Calculations

The conversion percentage (X_A%) of C_3H_8 and CO_2 was calculated using the below equation (12), when the fractional change in the volumetric flow rate was in consideration [51].

$$X_A(\%) = \frac{C_{in} - C_{out}}{C_{in} + \varepsilon_A C_{out}} \times 100 \quad\text{...} \quad (12)$$

Here, X_A is the conversion of the reactant (C_3H_8 or CO_2), and C_{in} and C_{out} are the inlet and outlet concentrations of C_3H_8 or CO_2, respectively. On the other hand, ε_A is defined as the below equation (13).

$$\mathcal{E}_A = \frac{\eta_{X_A=1} - \eta_{X_A=0}}{\eta_{X_A=0}} \quad\text{...} \quad (13)$$

Here, $\eta_{X_A=0}$ refers to the number of moles of reactants (no conversion) and $\eta_{X_A=1}$ is the number of moles of products (complete conversion). For the reactants gas composition of C_3H_8 (10%), CO_2 (30%), and Ar (60%), and ε_A is calculated to be 0.6 by using the aforementioned equations (13).

Chapter IV

Results and discussion

In this chapter, experimental results are discussed with proper explanations and figures. The first section will briefly discuss about the fresh catalysts (before reforming reactions) characterization and then the next sections will describe the catalytic performance on plasma catalytic dry reforming of propane reactions and the analysis of the carbon formation structure on the catalytic surface after reforming.

4.1 Characterization of the catalyst before reaction

4.1.1 TEM analysis:

TEM technique usually provides very useful information on the internal structure of materials using state art technology and it is considered an ideal instrumentation technique for morphological, compositional and crystallographic analysis. TEM analysis was carried out for both plasma-reduced and thermally reduced catalysts before reforming reaction to observe the surface morphology and microstructure shown in figure 21 (a - d).

36
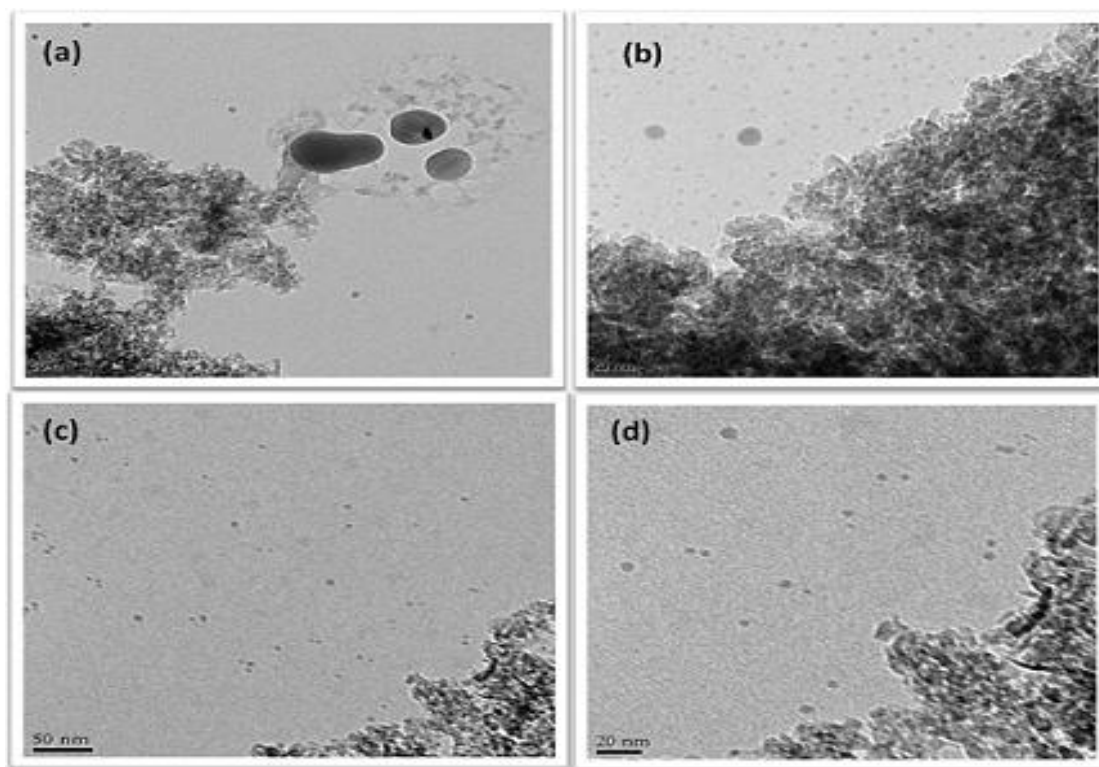
Figure.21: TEM images of thermally reduced (a & b) and plasma reduced (c and d) 4 wt%. Ni-CeO$_2$-γ/Al$_2$O$_3$ catalysts with different magnification.

In figure 21 (a - d), the dark spots reveal the active catalytic materials where the average particle diameter (dark spot) lies in the range of 3-40 nm and 3-5 nm for thermally and plasma reduced catalysts, respectively. According to the TEM analysis, the active particle diameter of the plasma reduced catalyst was much smaller compared to thermally reduced catalyst though it's difficult to distinguish the particles' diameter explicitly in the attached figures. In the case of thermally reduced catalyst, large Ni and ceria particles were poorly dispersed over the γ/Al$_2$O$_3$ support material. In contrast, the ultra-fine Ni nanoparticles were well dispersed over the γ/Al$_2$O$_3$ support material when the catalyst was reduced with plasma technique. In addition, plasma reduced catalyst was very stable even at high reaction temperature in consideration with this research work (600^{0}C).

However, the plasma based reduction technique has assisted to make ultrafine Ni and Ce nanoparticles with well dispersion on metal support compared to thermal reduction without sintering

and conglomeration, because high energetic electrons generated from plasma collided on the surface of catalyst to break the bond between metal oxides' (NiO and CeO$_2$) which resulted in small metal active sites (Ni and Ce).

4.1.2 SEM analysis:

SEM is a very useful and well established microscopic technique for local micro-chemical and morphological analysis in different materials. In addition, this technique can easily provide various signals from the catalyst surface using a high energy focused electron beam. In general, the obtained signals from SEM can deliver very authentic information on the surface overview in nano-scale regime with the approximation of crystal/grain size for proper understanding and better insights about catalyst surface including chemical composition, surface morphology, crystalline structure and orientation. In figure 22 (a - b), the surface overview of thermally and plasma reduced catalysts is demonstrated. In Fig- 22(a), it is clearly seen that the alumina support is consisted of loosely bounded nanoparticles of several nanometers in size (200 nm) in the case of thermally reduced catalyst; however, Fig-5(b) represents few nanometers size (80nm) nano-particles are strongly bounded with alumina support material for plasma reduced catalyst. Moreover, the plasma reduced catalysts' nanoparticles are well dispersed in comparison with thermally reduced catalyst due to plasma induced energetic electrons' bombardment effects on catalysts surface.
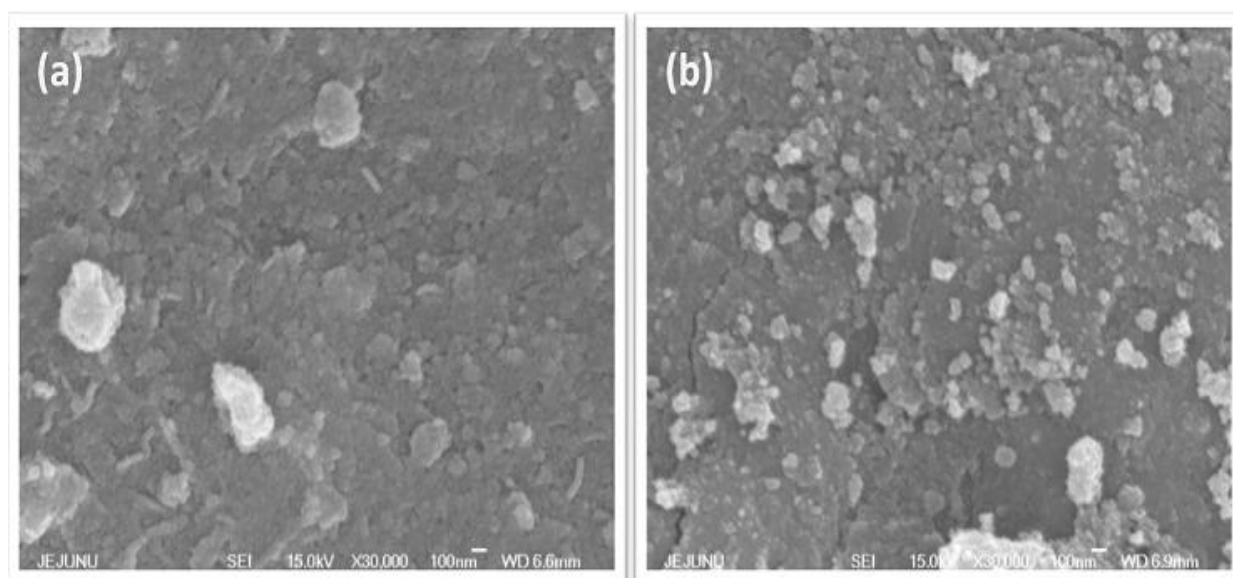
Figure.22: SEM images of fresh 4 wt.% Ni-CeO$_2$-γ/ Al$_2$O$_3$ (a) Thermally reduced catalyst and (b)

Plasma reduced catalyst before reforming reactions.

4.1.3 Powder X-ray diffraction:

X-ray diffraction (XRD) is a unique analytical method used for phase identification of crystalline materials and it demonstrates a "diffractogram" in terms of the intensity as a function of the diffraction angles. In Figure 23 (a - d), the XRD patterns of bare -γ/Al$_2$O$_3$ and 10 wt% Ni-CeO$_2$-γ/Al$_2$O$_3$ catalysts (general calcined, thermally and plasma reduced) before reforming reaction are demonstrated with different phase formation. In fact, this XRD based analysis was conducted using 10 wt% of Ni-CeO$_2$-γ/Al$_2$O$_3$ content instead of 4 wt% Ni-CeO$_2$-γ/Al$_2$O$_3$ to clearly understand the phase formation of metal converted from metal oxides because XRD technique cannot detect the phase formation of metal at low metal concentration.

In Fig. 23 (a), the bare -γ/Al$_2$O$_3$ phase diffraction peaks at 37, 46 and 67° are observed only. The CeO$_2$ phase diffraction peaks positioned at 28.5, 33, 47 and 56° are noticed in general calcined, thermally and plasma reduced catalysts and the NiO phase diffraction peaks are observed at 37, 45 and 61° overlapped with the γ-Al$_2$O$_3$ surface in all the reduced catalysts shown in Figure 23 (c - d). However, the presence of CeO$_2$ with higher intensities as a dominant factor in Figure 23 (b - c) indicates the lower content of NiO and Ni, and the strong interaction among NiO, Ni and support material shown in Figure 23 (b - c) [45]. On the other hand, the Ni phase strong diffraction peaks at 44.6, 51.9 and 76° can be ascribed to the successful conversion of NiO into Ni nanoparticles with well dispersion on catalyst surface by the plasma reduction where the content of CeO$_2$ and NiO are suppressed shown in Figure 23 (d). The aforementioned observations of the oxides and Ni formation prove that the strong coordination between the catalyst and the support resulted in the uniform dispersion of the catalyst over the support [47].
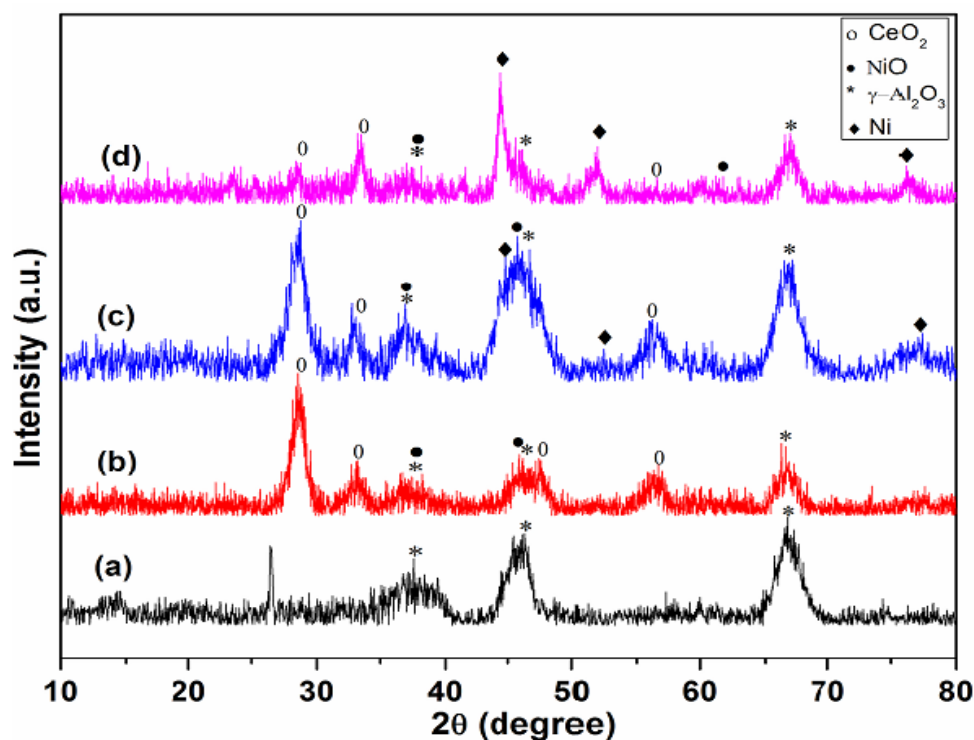
Figure.23: XRD patterns of (a) bare-γ/Al$_2$O$_3$, (b) general calcined 10 wt% Ni-CeO$_2$-γ/Al$_2$O$_3$, (c) thermally reduced 10 wt% Ni-CeO$_2$-γ/Al$_2$O$_3$ and (d) plasma reduced 10 wt% Ni-CeO$_2$-γ/Al$_2$O$_3$ catalysts before reforming reaction.

According to aforementioned systematic analysis, the plasma reduction resulted in relatively high dispersion of Ni nanoparticle over the support compared to general calcination and thermal reduction techniques. In addition, the correspondence of more Ni nanoparticles' reflections in plasma reduced catalyst represents that more active sites available for dry reforming reaction were formed which is due to plasma assisted reaction, because the plasma reduction technique is highly involved with the physical and chemical interactions between plasma and catalyst. According to the previous published research work [48], the discharge plasma can provide more active sites, high surface area, and strong metal/support interaction. The reduction of NiO to convert into Ni nanoparticles under H$_2$/Ar discharge plasma at low temperatures may undergo into several steps:

   i.   Electron (e$^-$) impact dissociation of H$_2$;

$$H_2 + e^- = H + H + e^- \tag{14}$$

   ii.   Adsorption and surface diffusion of hydrogen atom to the reduction center;

40

iii.   Breaking the Ni-O bond to form the metallic Ni nanoparticles;

$$NiO + H = Ni + OH \tag{15}$$

When the catalyst is exposed to plasma discharge, the catalyst particles work as the electron sinks and every catalyst particle can be charged up to thousands of electron volts (eV), and the trapped electrons usually create a plasma sheath around the particles. Furthermore, the plasma electron flow exerts a strong repulsive force on the generated sheath, and at the same time, a strong Coulomb repulsive force exists inside the trapped electrons. As a consequence, the energetic charged particles can easily be split by collisions with other energetic species which might result in high dispersion of Ni nanoparticles over the support and strong metal-support interaction [49]. After all, it is very clearly revealed that the metal oxides and metal Ni nanoparticles are well dispersed on the supported γ-Al_2O_3 surface due to the superior plasma reduction technique compared with other conventional techniques.

4.1.4 Raman Spectral Study

Raman spectroscopy is the most promising spectroscopic technique to observe vibrational and rotational transitions in molecular level [50]. In addition, this technique is widely used in chemistry to identify molecules, chemical bonding and crystallographic orientation of different materials. Raman spectroscopic measurement was conducted to investigate the crystallinity and bonding nature of the synthesized and calcined catalyst before reduction over the spectral region between $100 - 1200$ cm^{-1} as shown in Fig 24. A small oxygen vacancy band observed at 638 cm^{-1} represents the successful incorporation of the trivalent metal ions into the Ce_2O_4 lattice with the presence of Ce^{3+}. In addition, the stretching vibrational Raman band at 456cm^{-1} reveals the true presence of NiO.
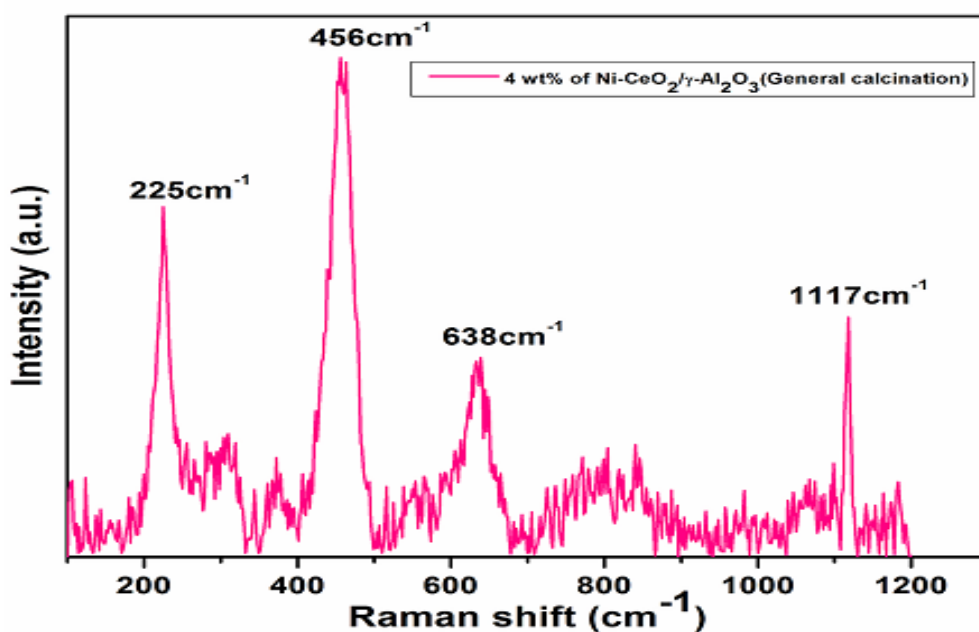
Figure.24: Raman spectra of fresh 4 wt% of Ni-CeO$_2$-ɤ/Al$_2$O$_3$ catalyst after general calcinations.

On the other hand, the additional Raman bands at 225cm^{-1} and 1117cm^{-1} are noticed which might be due to the stretching vibration of Ni-O or related defects on catalytic surface [51]. However, further analysis about the reducibility of metal ions for thermally and plasma reduced catalysts obtained from the H$_2$-TPR profile measurement has been discussed in the TPR section (4.1.5).

4.1.5 TPR analysis

Temperature-programmed reduction (TPR) is a widely used technique for the characterization of solid metal oxides dispersed on a support to find the most efficient reduction conditions. TPR process represents quantitative information of the reducibility of the oxide's surface. In this process, a reducing gas mixture (typically 10% hydrogen diluted in argon or nitrogen gas) flows over the sample with programmed temperature rising at 5°C/min from room temperature to 800°C. In general, a thermal conductivity detector (TCD) is used to measure the change in the thermal conductivity of hydrogen gas stream when it is consumed at certain temperature due to reduction process. Then, the concentration of active gas using a level calibration can obtain from the TCD signal conversion and the yield of total gas consumption can be calculated from the integration of the area under the concentration vs. temperature (or time).

제주대학교 중앙도서관
JEJU NATIONAL UNIVERSITY LIBRARY

4.1.5.1 H$_2$-TPR analysis

In specific, the TPR technique provides the qualitative and quantitative information about the reproducibility of the catalyst surface. In figure 25, TPR profile of the catalysts with Ni/Ceria contents of 4 wt% supported on γ-Al$_2$O$_3$ is depicted. In figure 25 (b), the thermally reduced catalyst shows broad reduction peaks at 286°C and 351°C which is indicating the reduction of NiO with moderate interaction with the support and other small peaks at 511°C and 628°C due to the smaller TPR signal of CeO$_2$ than the corresponding to the rest of the Ni/ceria-doped catalyst, respectively. The plasma reduced catalyst demonstrates broad main peaks at 440°C and 596°C shown in figure 25 (a) with other small peaks at different temperatures similar to thermally reduced catalyst. In previous studies, TPR analysis of pure CeO$_2$ demonstrated two peaks around at 500°C and 800°C. In addition, the plasma reduced catalyst's profile shows a broad peak at around 596°C corresponding to the reduction of bulk Ce^{4+} to Ce^{3+} for the case of CeO$_2$ reduction and another one broad peak at temperature 440°C may be attributed to the reduction of NiO to Ni metal.
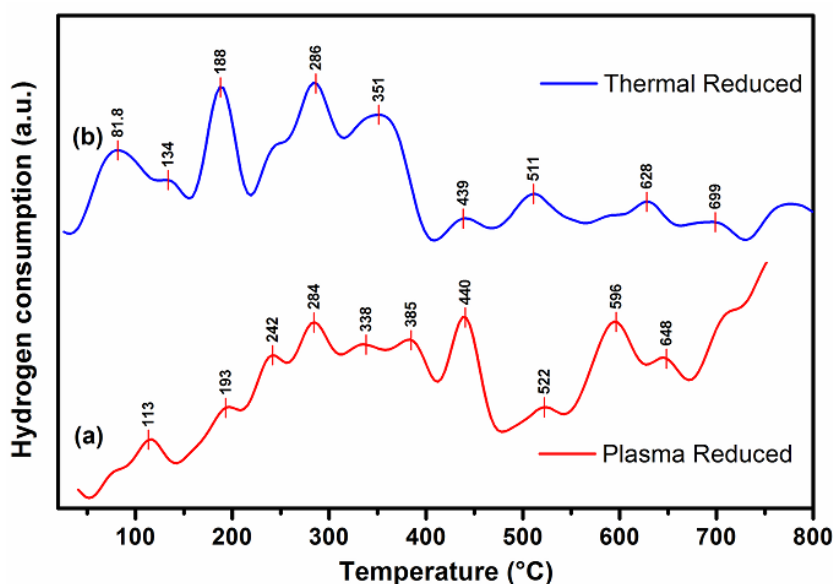
Figure.25: H2-TPR profiles of 4 wt% Ni-CeO$_2$-γ/Al$_2$O$_3$ catalyst: (a) thermal reduced and (b) plasma reduced.

Furthermore, both TPR profiles demonstrate few initial peaks at lower temperature due to the reduction of surface O_2 and bulk phase lattice O_2 of prepared $Ni\text{-}CeO_2\text{-}\gamma/Al_2O_3$ catalysts. Therefore, it seems that the complete reduction of Nickel, bulk and surface oxygen occurs simultaneously.

4.2 Chemical Characterization of the Active Sites

4.2.1 TPD analysis:

Temperature-Programmed Desorption (TPD) determines the number, type and strength of active sites available on the surface of a catalyst from the measurement of the amount of gas desorbed at various temperatures. In this analysis, the sample has been degassed at 250°C for at least 1 hour by passing Ar (45 ml/min) to take out the moisture and other adsorbed gases from surface and pores of the catalyst and then it has been cooled down to room temperature with the flow of Ar gas. After that, 10% of absorbent gases such as H_2 or CO_2 with a carrier gas (90% Ar) has passed through the prepared catalysts at the total flow rate of 50 ml/min for 30 min to absorbs on the active sites. Then, the H_2/CO_2 flow was turned off and adsorbed gases were purged with pure Ar flow for 30 min. In TPD pattern, the temperature increased linearly with time up to 800°C at a rate of 10°C/min while the desorption of H_2 was monitored (Figure 26). In general, the heat overcomes the activation energy after certain temperature; as a result, the bond between the adsorbate and adsorbent breaks easily when the adsorbed species desorbed. If different active metals are present during TPD analysis, the adsorbed species are usually desorbed at different temperatures. Then, desorbed species enter the stream of carrier gas (Ar) and are swept to the detector, which measures the gas concentrations (mol/L) vs. time. Finally, the area is calculated from the read out of detector (gas concentrations vs. time). However, the area corresponds to the number of desorbed species/molecules (mol).

4.2.1.1 H_2-TPD analysis

H_2-TPD curves for 4 wt%. of $Ni\text{-}CeO_2\text{-}\gamma/Al_2O_3$ catalysts prepared by various methods shown in Figure 26.
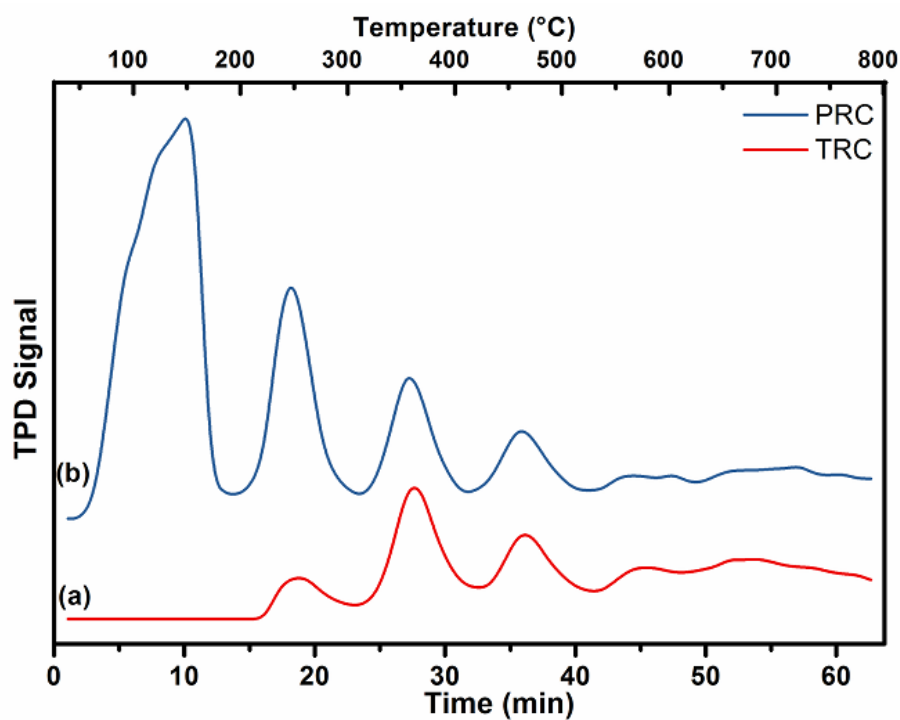
Figure.26: H_2-TPD patterns of 4 wt%. of Ni-CeO$_2$-γ/Al$_2$O$_3$ catalysts: (a) TRC and (b) PRC.

Fig. 26 (b) shows a very strong bound chemisorptions site at 164°C, whereas few chemisorbed sites at the same temperature with very low concentration is still in detection shown in Fig. 26 (a). In Fig. 26 (a and b), the chemisorbed hydrogen amount increase in accordance with the order of Ni-CeO$_2$-γ/Al$_2$O$_3$ (TRC) and Ni-CeO$_2$-γ/Al$_2$O$_3$ (PRC), which shows that the plasma reduced catalyst (PRC) has the largest hydrogen adsorption capacity. On the other hand, the thermally reduced catalyst presents very less amount of hydrogen adsorption capacity. Table 6 demonstrates the number of active sites which is calculated according to the TPD spectra.

Table 6: number of active sites.

Samples	Number of active sites in gram
Ni-CeO$_2$-γ/Al$_2$O$_3$ (TRC)	1.99503E+20
Ni-CeO$_2$-γ/Al$_2$O$_3$ (PRC)	4.70523E+20

The above results reveal that the plasma based process has greatly improved the hydrogen adsorption capacity of Ni-CeO$_2$-γ/Al$_2$O$_3$ (PRC) catalyst, and increased more active sites on the catalysts surface compared to thermally reduced catalyst. In TRC preparation most of the metallic particles were easily sintered and conglomerated due to the long time (6 h) calcination and reduction at high temperature (500°C); however, the PRC contains large amount of H atoms and other high energetic particles due to the plasma based process which can easily decompose the precursor and convert the metal oxides to metal active sites. In DBD plasma reactor, the energetic charge particles bombard on the catalyst surface which creates more active sites with well dispersion and also it can avoid the unexpected sintering of metallic particles [52]. Therefore, the TPD results confirm the formation of active sites for plasma based reduction technique, which is well agreed with the results of XRD characterization.

4.2.1.2 CO$_2$-TPD analysis

In Fig. 27 (a and b), CO$_2$-TPD curves for 4 wt% of Ni-CeO$_2$-x/Al$_2$O$_3$ catalysts prepared by two methods are presented where both catalysts show a weak Lewis alkaline site adsorbed at low temperature around 100-150°C in initial time. On the other hand, a strong Lewis alkaline site adsorbed at 300–500°C is observed. The number of active sites' dispersion data calculated according to the CO$_2$-TPD spectra of two samples is listed in Table 7.

Table 7: number of active sites.

Samples	Number of active sites in gram
Ni-CeO$_2$-γ/Al$_2$O$_3$ (TRC)	3.93708E+21
Ni-CeO$_2$-γ/Al$_2$O$_3$ (PRC)	4.90028E+21

According to the aforementioned results, the peak area of Ni-CeO$_2$-γ/Al$_2$O$_3$ (TCR) catalyst are smaller compared to Ni-CeO$_2$-γ/Al$_2$O$_3$ (PCR) catalyst and the number of active sites are greater in plasma reduced catalyst than the thermally reduced catalyst. According to Li et al., CO$_2$ adsorption occurs generally on the support surface instead of on the Ni particle because it can be adsorbed on the alkaline side of the support surface. The increase of CO$_2$-TPD peak area reveals that the plasma based

technique has improved the alkalescence of support surface significantly. Therefore, the catalyst surface is benefited for the carbon deposition elimination with increased coking-resistant ability.
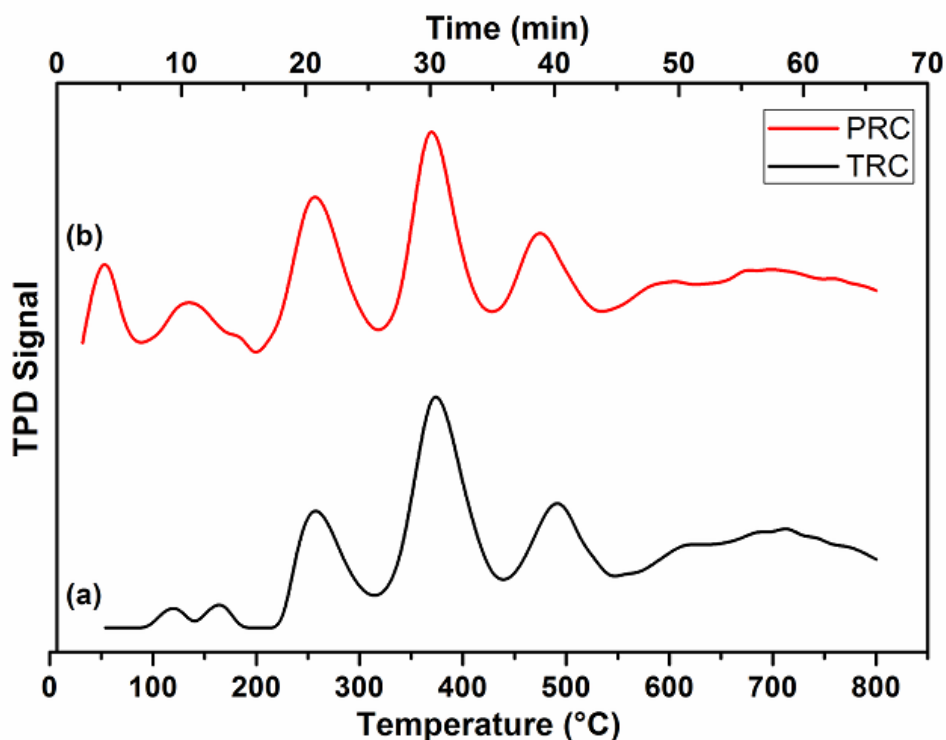
Figure.27: CO_2-TPD patterns of the 4 wt%. of Ni-CeO$_{2-}$γ/Al$_2$O$_3$ catalysts: (a) TRC and (b) PRC.

4.3 Dry Reforming of Propane (DRP)

Plasma catalytic dry reforming of C_3H_8 is conducted with plasma reduced and thermally reduced catalysts (Ni-CeO$_{2-}$γ/Al$_2$O$_3$) using the reactants gas mixing ratio of 1:3 (C_3H_8/CO_2) with a total flow rate of 300 ml min^{-1}. The major desired products of dry reforming reaction are H_2 and CO, whereas small amounts of methane and carbon dioxide production are also observed in GC (gas chromatography). The catalytic activity in terms of propane and CO_2 conversion was evaluated in the temperature range of 500-600°C at 20°C intervals in the dry reforming process. To investigate the influence of plasma assisted reaction mechanism on catalytic activity for both plasma reduced and thermally reduced catalysts, DRP process was conducted in four different ways such as TRC, TRC + Plasma, PRC and PRC + Plasma shown Fig. 28 (a and b).

제주대학교 중앙도서관
JEJU NATIONAL UNIVERSITY LIBRARY
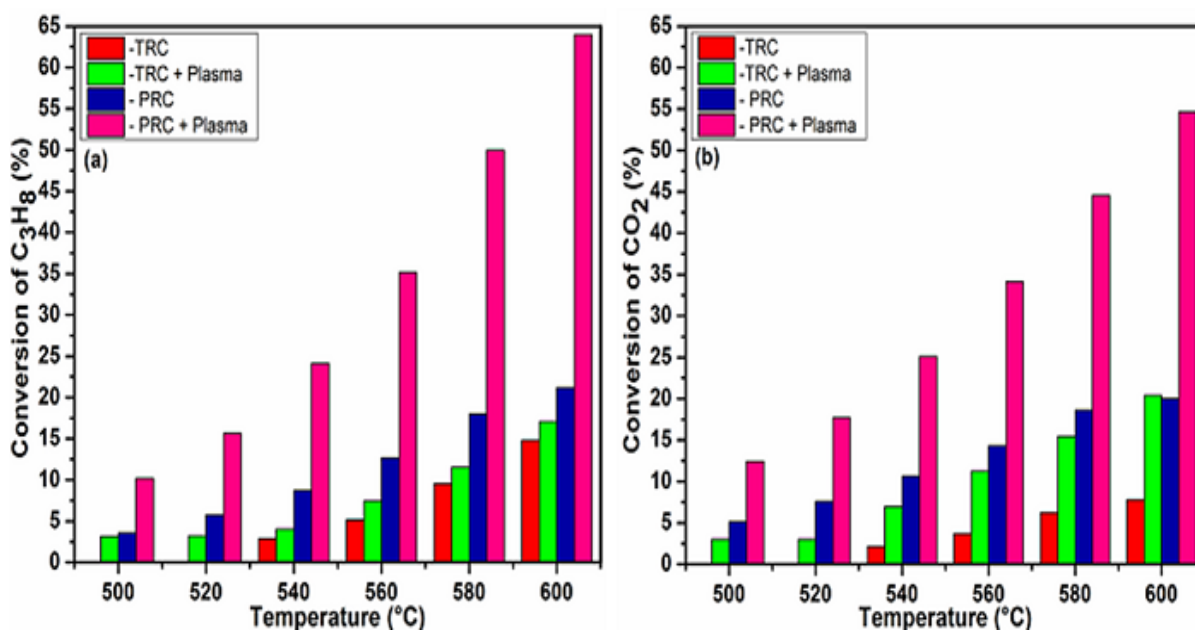
Figure.28: Conversion at different temperatures: (a) C_3H_8 and (b) CO_2.

In Fig. 28 (a and b), the percentage of conversion for both propane and CO_2 has linearly increased with the increase of the temperature. The conversion efficiencies of C_3H_8 and CO_2 are 14.79, 17.07, 21.18 and 64.01%, and 7.79, 20.41, 19.27 and 54.64% for the TRC, TRC + Plasma, PRC, and PRC + Plasma catalysts at 500, 520, 540, 560 580 and 600°C, respectively. Among the four types of conducted DRP process, the PRC + Plasma based DRP process has demonstrated better catalytic performance compared to other three processes, which is due to its superior catalytic activity that can be attributed to the double effect of plasma reduction. In fact, the double effect of plasma based catalyst reduction in the DRP process initiates the formation of ultra-fine active nano-crystals and active phases with uniform dispersion over the support material which usually improves the catalytic activity. On the other hand, the increase of temperature also improves the conversion rate by increasing the mobility of lattice oxygen atoms in the reforming reactions [53]. According to the conducted study, the PRC + Plasma based DRP process could be a leading reaction mechanism for its higher catalytic activity and lower carbon deposition on the catalyst surface during dry reforming reaction. Furthermore, the C_3H_8 conversion was 10 % higher than the CO_2 conversion, which is due to the high mobility of activated lattice oxygen on the surface of supports and the reaction of activated

48

oxygen with propane in the gas phase [54]. Among the all catalytic process, TRC process has exhibited a relatively poor performance even at high temperature (600°C) due to the formation of coke over the surface of catalyst. Furthermore, we could not observe any conversion below at 540°C temperature due to carbon deposition proceeding via propane dehydrogenation or the Boudouard reaction equation (Eq. (8) and Eq. (9)), respectively.

$$C_3H_8 \rightarrow 2C + CH_4 + 2H_2 \tag{14}$$

$$2CO \rightarrow C + CO_2 \tag{15}$$

During the plasma catalytic dry reforming, both PRC and TRC catalysts have shown better catalytic activity compared to thermally reduced catalyst only. Therefore, plasma is a very useful technique to increase the catalytic activity compared to conventional techniques for DRP process in terms of conversion efficiency. In fact, plasma based catalytic reactions generally produce huge number of energetic electrons with Ni active sites while ceria plays a role as a promoter in Ni-rich materials with their stability improvement, and the reducible nature of Ni active sites contributes to the improvement of catalytic activity. These findings lead us to suggest that the physical and chemical interactions between plasma and catalyst may be responsible for the better performance in reforming reaction.
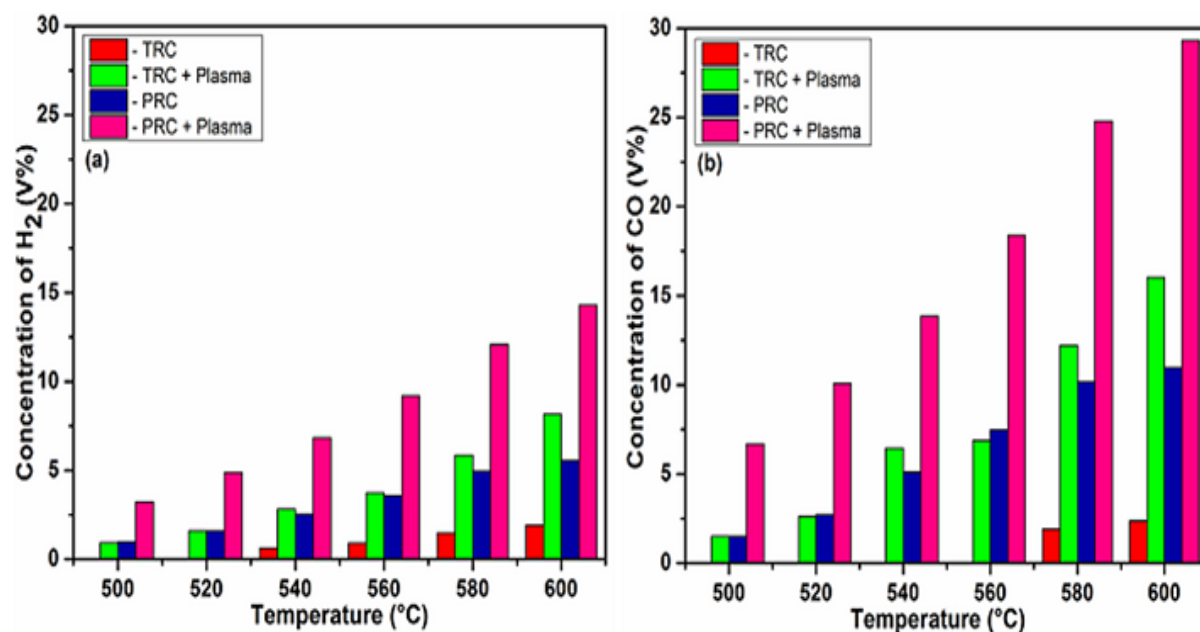

Figure.29: Concentrations of H_2 and CO obtained with different catalysts.

The measured concentrations of H_2 and CO for four types of DRP process are shown in Fi. 29 (a and b), where it can explicitly be seen that the concentrations of both H_2 and CO obtained with the PRC + Plasma catalytic process are much higher compared to others process. According to the obtained results (Fig. 29 (a and b), The TRC process has produced very less amount of H_2 and CO compared to the others three process. On the other hand, the production of H_2 and CO for the PRC + Plasma catalytic process has increased to 14 vol% and 29 vol% , respectively, which is due to plasma induced reaction mechanism on the catalytic active sites. The enhancement of plasma reduced catalytic activity for DRP process could be due to the ultrafine Ni nanoparticles' creation with well dispersion over the support material. The concentration of CO is higher than that of H_2 for all the four types DRP process and the product concentrations has increased with the increase of temperature from 500 to 600°C as DRP is a endothermic reaction [55]. The H_2/CO ratio is lower than the theoretical value, 0.6, which might be due to side reactions such as the reverse water gas shift (RWGS) (Eq. (16) reaction, viz.

$$CO_2 + H_2 = CO + H_2O \qquad\qquad (16)$$

It is well agreed that the metal-oxygen species formation on ceria surface with the interaction between metal and CeO_2 generally increase the stability and dispersion of metal. In this investigation, plasma reduced catalyst with plasma aided reaction mechanism (PRC + Plasma) for DRP process has demonstrated comparatively higher catalytic activity with a large number of active sites creation and lower carbon deposition.

4.3.1 Best Catalytic Performance with Applied Voltage in DRP

In this section, the catalytic performance of PRC + Plasma based DRP process has been discussed with respect to the discharge power and applied voltage to analyze the reactants' conversion (%) and products' concentration (vol%). The effect of applied voltage on the plasma assisted catalytic reaction has been analyzed with the variation of the voltages from 6 to 10 kV shown in shown in Fig. 30 (a - c). In this experiment, the minimum voltage was around 3 kV and the plasma formation was very weak at this voltage. Therefore, the catalytic activities were evaluated at 600°C from 6 to 10.3 kV

50

applied voltage with 1 kV interval. The maximum voltage around 10.3 kV has demonstrated the best catalytic performance in terms of conversion and concentration efficiencies compared to others applied voltage. The discharge power and applied voltage for the observed DRP reactions were 0.6277, 1.5578 and 2.6314 W, and 6.1, 8.1 and 10.3 kV, respectively. According to the conducted analysis, the conversion of both C_3H_8 and CO_2 has linearly increased with the increase of discharge power as shown in Fig- 30 (b & c), because an increase in plasma power produces more active species/radicals with higher degree of ionization of reactants gas which ultimately increase the production of syngas. Radicals can be generated due to the collision of energetic electrons with neutral molecules at certain applied voltage depending on the reactor geometry and gas composition [56].

Figure.30-(a) Discharge power vs applied voltage, and Fig. 30-(b, and c) conversions (%) and concentrations (V%) of DRP process respect with discharge power.

51
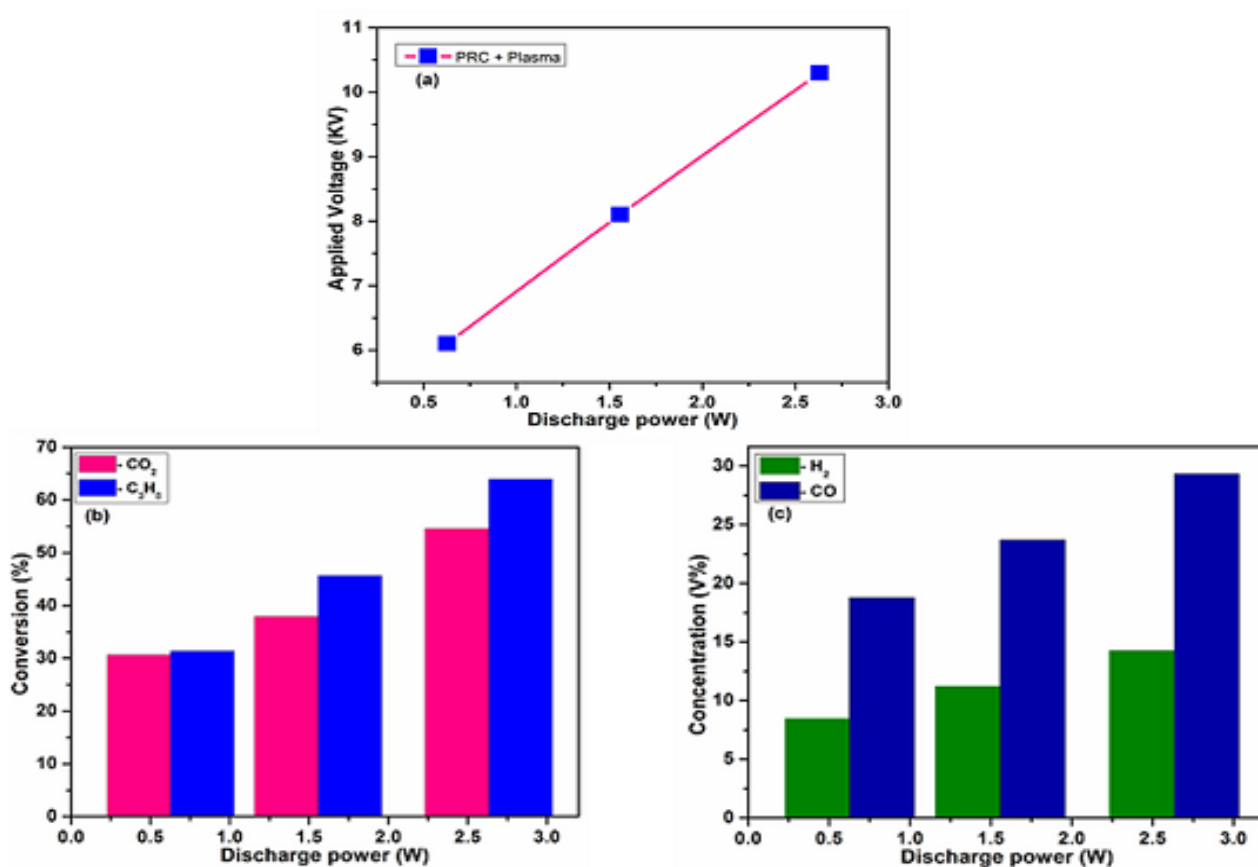
4.4 Characterization of the catalyst after reaction

The structural and phase modifications of the catalysts after the dry reforming reaction were further investigated using Raman spectroscopy and SEM. The following two sub-sections will discuss about the structural and phase modifications of used catalysts in dry reforming reaction.

4.4.1 SEM analysis

The SEM analysis of all the used catalysts for the DRP was carried out to confirm the carbon deposition and its microstructures, which is shown in Figure 32 (a - d). As observed in SEM images, carbon formation with various forms on catalyst surface are observed clearly after the dry reforming reaction. Carbon whiskers were observed for the TRC, TRC + Plasma and PRC + Plasma catalysts from higher diameter to lower diameter, respectively; on the other hand, very fine flaky carbon was deposited on the PRC catalyst. So, the amount of carbon deposition is less on the surface of plasma reduced catalyst compared to thermally reduced catalyst, while the appearance of the carbon formation on the TRC, TRC+ plasma and PRC + plasma catalysts' surface are almost similar. The huge amount of carbon whiskers' formation on the thermally reduced catalyst could destroy the catalyst structure, eventually decrease the catalytic activity.

According to the aforementioned analysis, plasma based technique has a great impact on catalyst surface to reduce the carbon formation and keep long-term stability during DRP compared to existing conventional techniques. The observed discrepancies in the carbon formation structure on catalysts surface might be due to the variation in the reaction kinetics during dry reforming reaction [57].
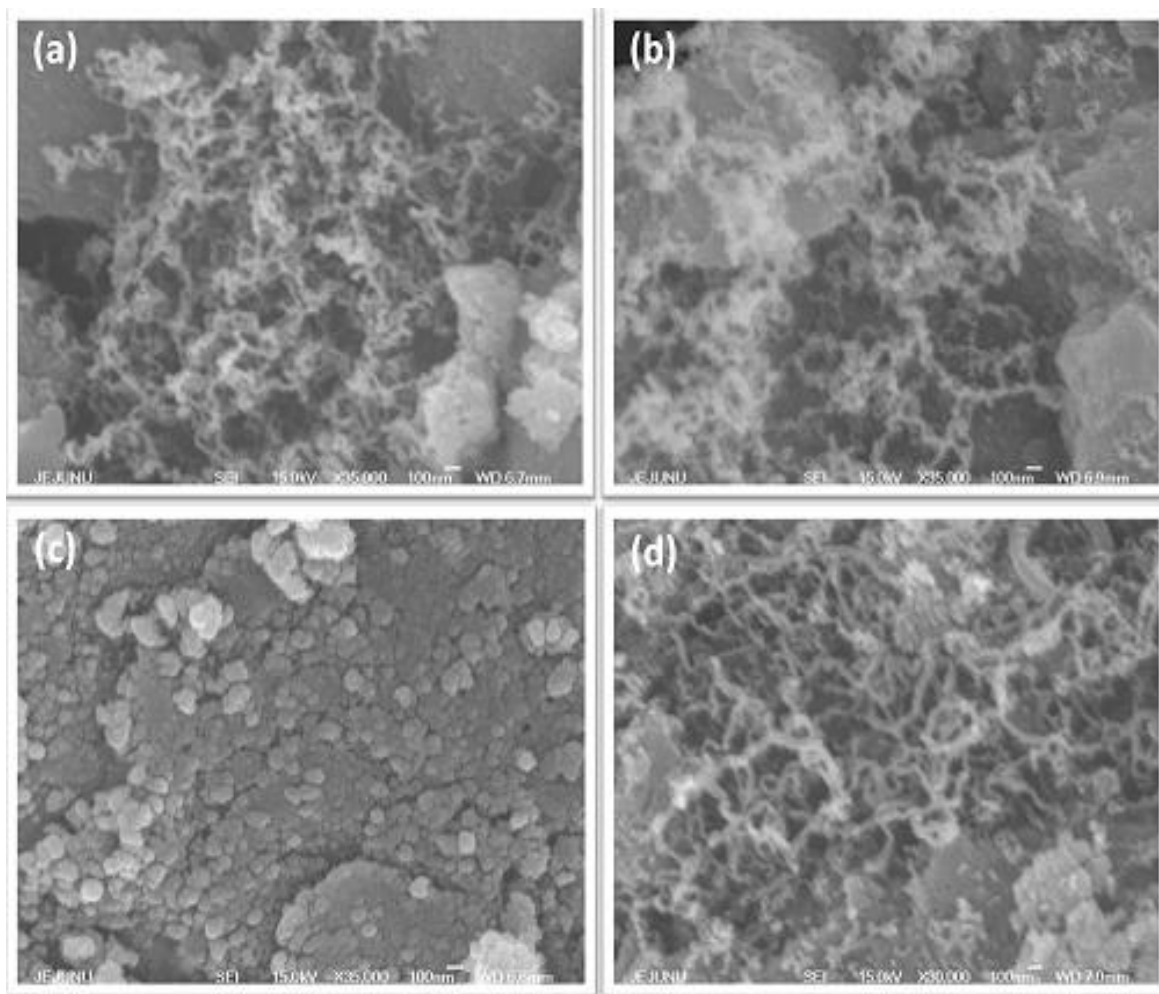
Figure.31: SEM images of 4 wt.% Ni-CeO$_2$/γ-Al$_2$O$_3$ catalysts after reforming reaction: (a) TRC, (b) TRC + Plasma, (c) PRC and (d) PRC + Plasma.

4.4.2 Raman spectroscopy

Raman spectroscopic technique is a well-established tool to identify the internal chemical structure and the presence of carbonaceous elements on the catalyst surface after dry reforming reaction and it can also provide the specific information about the nature of carbonaceous deposits (coke). In figure 33 (a - d), Raman spectroscopic analysis has revealed the nature of carbon species explicitly over the catalysts surface after the dry reforming reaction.

Two sharp major bands at 1344 cm^{-1} (D band) and 1600 cm-1 (G band) are observed for all the used catalysts from the Raman spectroscopic measurement, where the first peak (1344 cm^{-1}) is associated with the disordered sp^2 - bonded hybridized carbon atoms. On the other hand, the second peak at 1600

53

cm^{-1} is attributed to the E_{2g} vibration mode of graphite in the two-dimensional hexagonal lattice of the graphite layer which is formed during the dry reforming reaction. Furthermore, an additional peak at 2713 cm^{-1} (2D band) is observed for the thermally reduced Ni-CeO$_2$-γ/Al$_2$O$_3$ used catalyst, which substantiates the single-wall carbon nanotubes (CNTs) formation over the catalyst surface during dry reforming reaction shown in Figure 33-(a). So, the spectroscopic based obtained results aid to the proper understanding of the graphitization of carbon and the degree of disorder with regard to the relative intensity ratio (I_D/I_G) of the studied catalysts.

However, the PRC catalyst shows very low intense peak at 1344 cm^{-1} and 1600 cm^{-1} indicating the less amount of carbon deposition on the surface catalyst, which means that the catalyst surface remains active. In addition, the disordered sp^2 - bonded hybridized carbon atoms observed at Raman band 1344 cm^{-1} for thermally reduced catalyst proves the less catalytic performance. According to the aforementioned analysis, plasma reduced catalysts contain comparatively less small amount of carbon deposition on the catalyst surface compared to thermally reduced samples, which means that the surface of these catalysts remains active.
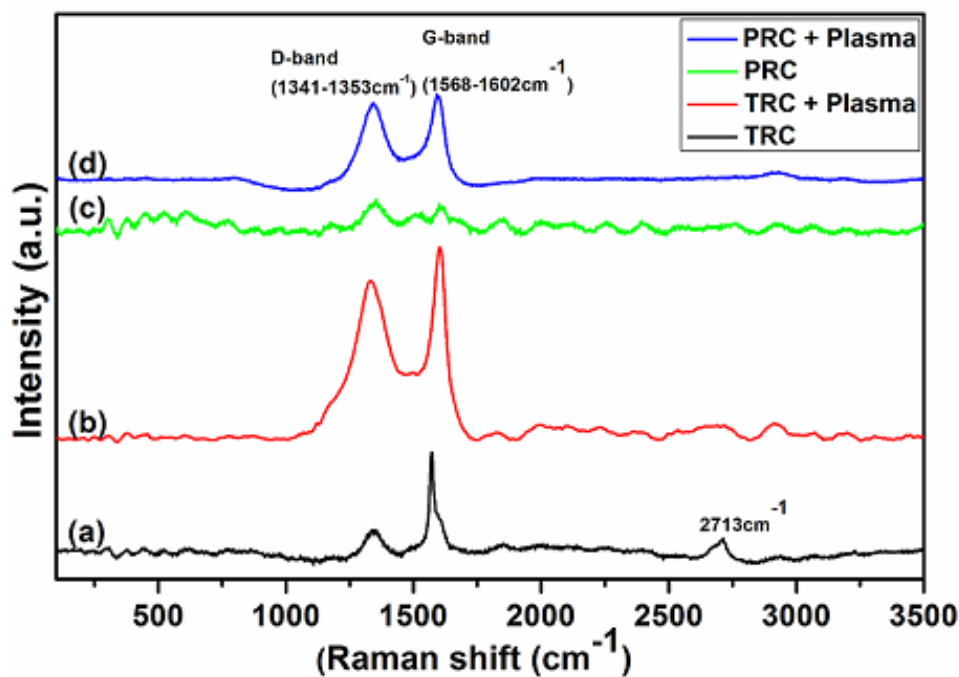

Figure.32: Raman spectra of 4 wt% Ni-CeO$_2$-γ/Al$_2$O$_3$ catalysts after dry reforming reaction: (a) TRC (b) TRC + Plasma, (c) PCR and (d) PRC + Plasma catalyst.

4.4.3. Temperature-Programmed Oxidation (TPO) analysis

Temperature-Programmed Oxidation (TPO) determines the amounts of carbon formation on spent catalysts after dry reforming reactions. In the conducted TOP analysis, the catalyst sample has been degassed at 600°C for around 30 min by passing N_2 (45 ml/min) to take out the moisture and other adsorbed gases from surface and pores of the catalyst. After that, 10% O_2 with a carrier gas (90% Ar) has passed over the prepared catalysts' surface at a total flow rate of 50 ml/min until removing all carbon contents from the used catalysts' surface at 600^0C. In general, the heat overcomes on the surface of spent catalysts and the deposited carbon was removed as a CO_2 gas. However, we didn't observe any CO gas peak from FTIR during oxidation. As a consequence, the flow of O_2 was turned off to calculate the area from the readout of FTIR-detector (gas concentrations vs. time), where the area corresponded to the amount of carbon deposition on spent catalysts' surface. In Fig. 33, the TPO profiles regarding with area of carbon deposition on spent catalysts (TRC, TRC + Plasma, PRC, and PRC + Plasma) are demonstrated.
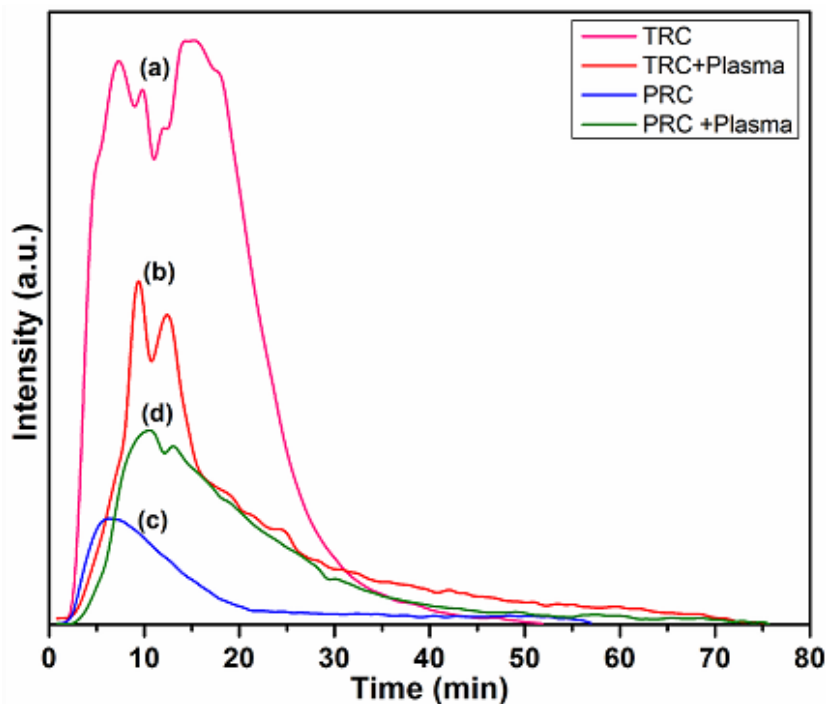

Figure 33: TPO profiles of spent catalysts: (a) TRC, (b) TRC + Plasma, (c) PRC and (d) PRC + Plasma.

According to the TPO profiles (Fig. 33), it is very clearly seen that the amount/area of carbon deposition is higher in thermally reduced (TRC and TRC + Plasma) catalysts compared to Plasma reduced catalysts (PRC and PRC + Plasma). In addition, the less carbon formation in plasma reduced catalysts for dry reforming reactions are also observed in SEM and Raman spectroscopic investigations, which is discussed in previous sections. The amount of carbon deposition in wt.% of spent catalysts are given in Table 8.

Table 8: Amount of carbon deposition in wt.%.

Catalysts	Carbon deposition in wt.%
TRC	7.5
TRC + Plasma	3.4
PRC	0.9
PRC + Plasma	2.4

The very less wt.% of carbon deposition on plasma reduced catalysts, 0.9 and 2.4 wt.% for PRC and PRC + plasma respectively, proves the plasma assisted best catalytic reaction mechanism for higher H_2 production. Therefore, the plasma reduced catalysts are more active and stable in all perspectives for DRP process including coke restive properties compared to thermally reduced catalysts.

Chapter V

CONCLUSIONS AND FUTURE DIRECTIONS

5.1 Conclusions

In this research, plasma catalytic dry reforming of propane to syngas has been conducted in a DBD reactor with plasma and thermally reduced 4 wt.% $Ni-CeO_2.\gamma/Al_2O_3$ catalysts which were prepared by the simple wet-impregnation method and characterized by various analytical techniques to confirm the catalytic performance accurately. The generation of highly active ultra-fine Ni metal nano-particles and rich ceria oxide phase with uniform dispersion on the catalyst surface were gained by the plasma-assisted DRP process for plasma reduced catalyst compared to others conducted process, which was confirmed by XRD, TPD and TEM analysis. The TPD and TEM analyzed results also confirmed that the plasma induced DRP process (PRC + plasma) produced only huge number of active sites with nano-scale regime (3 – 5 nm) during reforming reaction which enhanced the catalytic activity for better conversion efficiency. The Raman band at 638 cm^{-1} confirmed the presence of higher lattice oxygen with the incorporation of CeO_2, which can inhibit the coke formation on catalyst surface with the enhancement of catalytic activity. In addition, TPR analysis also observed a strong interaction between CeO_2 and nickel oxide surface layer on the support of plasma reduced catalyst which facilitated catalyst reduction comparatively at a lower temperature. Among the all evaluated catalytic process, PRC + Plasma based reforming reaction has showed the better catalytic activity with the highest C_3H_8 and CO_2 conversion to H_2 and CO production. In addition, the highest production of hydrogen in plasma catalytic dry reforming which approached that of a stoichiometric reaction was in favor to the minimal amounts of carbon deposition on catalyst surface with long time catalyst durability. On the other hand, thermally reduced catalyst has demonstrated very poor catalytic performance in terms of reactants conversion to products gas compared to plasma reduced catalyst which might be due to higher carbon deposition on catalyst surface. Therefore, it can be concluded that plasma reduced catalyst has exhibited better catalytic performance over thermally reduced

catalyst for its novel reaction mechanisms such as anti-coke sintering, creation of a large number of active sites and well dispersion of Ni active metallic nano-particles on catalyst surface.

After all, a systematic study is needed to optimize the plasma parameters (discharge gap, gas retention time, material of dielectric barrier and waveform of power supply) for higher catalytic activity in terms of maximum hydrogen production at lower reaction temperature and applied voltage.

5.2 Future works:

DRP is a unique process for syngas production due to the utilization of CO_2 as a feed gas that can potentially offset the increase of GHG emissions in the future days. The woks that could be explored are stated below:

i)   New catalytic materials will be explored for the best catalytic activity with coke resistance property and long-term durability.

ii) New types of plasma reactor will be investigated for optimum plasma-induced radical generation for maximum hydrogen production with less carbon deposition.

5.3 References

[1] Shiyi C. Energy Consumption, CO_2 Emission and Sustainable Development in Chinese Industry. Economic Research Journal, 2009-4.

[2] Ghorbani A, Jafari M, Rahimpour M R. A comparative simulation of a novel gas to liquid (GTL) conversion loop as an alternative to a certain refinery gas flare. Journal of Natural Gas Science and Engineering 2013; 11(0): 23-38.

[3] Tu X, Gallon H J, Twigg M V, Gorry P A, Whitehead J C. Dry Reforming of Methane over a Ni/Al$_2$O$_3$ Catalyst in a Coaxial Dielectric Barrier Discharge Reactor. J. Phys. D: Appl. Phys 2011; 44:27.

[4] Harling A M, Glover D J, Whitehead J C, Zhang K. Environ. Sci. Technol 2008; 42 **:**4546.

[5] Gallon Helen J. Dry Reforming of Methane Using Non-Thermal Plasma-Catalysis, PhDs Thesis, The University of Manchester, Manchester, USA, 2010.

[6] (BAU, 850.6 MtCO$_2$eq) Intended Nationally Determined Contribution, Submission by the Republic of Korea.

[7] EU and South Korea target closer cooperation on climate, carbon markets 25 September 2015.

http://www.decc.gov.uk/en/content/cms/what_we_do/change_energy/tackling_clima/emissions/eu_ets/eu_ets.aspx

[8] www4.unfccc.int/.../Republic%20of%20Korea%20First/INDC%20Submission%20. Republic of Korea first NDC.

[9] Chang J S, Lawless P A, Yamamoto T. Corona Discharge Processes. IEEE T. Plasma Sci. 1991; **19**(6):1152-66.

[10] Ferreira-Aparicio P, Rodríguez-Ramos I, Anderson J A, Guerrero-Ruiz A, Mechanistic. Aspects of the Dry Reforming of Methane Over Ruthenium Catalysts. Appl. Catal. A, 2000; 202(2):183-196.

[11] Hu Y H. Solid-Solution Catalysts for CO$_2$ Reforming of Methane. Catal. Today 2009; **148**(3-4):206-211.

[12] Kong Zi Ying. Thermodynamic Analysis of Methane Dry Reforming, BSc Thesis, Universiti Malaysia Pahang, Pahang, Malaysia, 2013.

[13] Silvestri G, Gambino S, Filardo G. Electrochemical Syntheses Involving Carbon Dioxide. Springer 1990; 314:101-127.

[14] Wender I. Reactions of synthesis gas. Fuel processing Technology, Elsevier 1996; 48:189-297.

[15] Rostrupnielsen J R, Hansen J H B. CO_2-Reforming of Methane over Transition Metals. Journal of Catalysis1993; 144: 38-49.

[17] Wilhelm D J, Simbeck D R, Karp A D, Dickenson R L. Syngas Production for Gas-to-Liquids Applications: Technologies, Issues and Outlook. Fuel Process. Technol 2001; 71:139-148.

[19] Collodi G, Wheeler J. Hydrogen Production via Steam Reforming with CO2 Capture. Chemical Engineering Transactions 2010; 19:37-42.

[20] Fidalgo B, Menendez J A. Carbon Materials as Catalysts for Decomposition and CO2 Reforming of Methane. Chinese Journal of Catalysis 2011; 32(2):207-216.

[21] Fan M S, Abdullah A Z, Bhatia S. Catalytic Technology for Carbon Dioxide Reforming of Methane to Synthesis Gas. ChemCatChem 2009; **1**(2):192-208.

[22] Kraus M. Catalytic CO_2 Reforming of Methane in a Dielectric-Barrier Discharge. Phys. Chem. Chem. Phys 2001**;** 3:294-300.

[24] Song, C. Tri-reforming: A new process for reducing CO_2 emission. Chemical Innovation 2001, 31(1), 21-26.

[25] FETC (Federal Energy Technology Center). Vision 21 Program Plan - Clean Energy Plants for the 21st Century. Office of Fossil Energy, U.S. Department of Energy, Washington, D.C., 1999.

[26] Pan W, Zheng J, Song C. Catalytic Tri-reforming of Methane Using Flue Gas from Fossil Fuel-based Power Plants. Fuel Chemistry Division Preprints 2002; 47(1), 262.

[27] Song, C, Pan W. Tri-reforming of methane: a novel concept for catalytic production of industrially useful synthesis gas with desired H_2/CO ratios. Catalysis Today, 2004. 98(4): p. 463-484.

[28] Li, Y. Thermodynamic analysis of autothermal steam and CO_2 reforming of methane. International Journal of Hydrogen Energy, 2008. 33(10): p. 2507-2514.

[29] Amjed A, Hassani A, Hazzim F, Abbas, W M A, Daud W. Hydrogen production via decomposition of methane over activated carbons as catalysts: Full factorial design Int. J. Hydrogen Energy 2014; 13 (39) : p.7004-7014.

[30] Asztalos Z T, Lucaci A I, Cormos C C, Agachi P S. Thermodynamic Study of Hydrogen Production via Bioglycerol Steam Reforming. Computer Aided Chemical Engineering 2014; 33:1735-1740.

[31] Kale G R, Gaikwad T M. Thermodynamic Analysis of Ethanol Dry Reforming: Effect of Combined Parameters. International Scholarly Research Notices; 2014.

[32] Kalai D Y. Dry reforming of methane: catalyst development and thermodynamic analysis. The University of Stavanger 2015.

[33] Chen F F. Introduction to Plasma Physics and Controlled Fusion. Springer; 2nd Edition, 1984.

[34] Trinh Q H, Mok Y S. Environmental plasma-catalysis for the energy-efficient treatment of volatile organic compuonds. Korean Journal of Chemical Engineering 2016; 33:735-748.

[35] https://www.livescience.com/54652-plasma.html.

[36] http://www.sciencedirect.com/science/article/pii/S0360319908013955.

[37] Zou J J, Zhang Y P, Liu C J. Reduction of Supported Noble-Metal Ions Using Glow Discharge Plasma. American Chemical Society, Langmuir 2006; 22 (26), pp 11388–11394**.**

[38] https://en.wikipedia.org/wiki/Glow_discharge.

[39] Nguyen D B, Park J N, Lee W G. Conversion reaction of methane with carbon dioxide in glow discharge at atmospheric pressure. Journal of the Korean Industrial and Engineering Chemistry 2014; 25(5):497-502

[40] Ahmar E E, Met C, Aubry O, Khacef A, Cormier J M. Chem. Eng. J.2005; 116-13.

[41] El-Aragi G M. Gliding Arc Discharge (GAD) Experiment, Plasma Physics and Nuclear Fusion Dept., Nuclear Research Center, AEA, PO 13759 Cairo, Egypt.

[42] Liu G H., Li Y L, Chu W, Shi X Y, Dai X Y, Yin Y X. Plasma-Assisted Preparation of Ni/SiO$_2$ Catalyst Using Atmospheric High Frequency Cold Plasma Jet. Catal. Commun 2008; 9(6): p. 1087-1091.

[43] Conrads H, Schmidt M. Plasma Generation and Plasma Sources. Plasma Sources Sci. T 2000; **9**(4): p. 441-454.

[44] Eliasson B, Kogelschatz U. Nonequilibrium Volume Plasma Chemical-Processing. IEEE T. Plasma Sci 1991; 19(6): p. 1063-1077.

[45] Yu. A. Lebedev, Microwave discharges at low pressures and peculiarities of the processes in strongly nonuniform plasma, Plasma Sources Science and Technology 2015; 24(5):053001.

[46] Jimenez-Gonzalez C, Boukha Z, de Rivas B, Delgado J J, Cauqui M A, Gonz_alez-Velasco J R. Structural characterisation of Ni/alumina reforming catalysts activated at high temperatures. Appl Catal A 2013;466:9-20.

[47] Wang S, Lu G Q. Role of CeO$_2$ in Ni/CeO$_2$-Al$_2$O$_3$ catalysts for carbon dioxide reforming of methane. Appl Catal B 1998;19:267-77.

[48] Terashima K, Howald L, Haefke H, Guentherodt H. Development of a mesoscale/nanoscale plasma generator. Thin Solid Films 1996;281:634-6.

[49] Liu C J, Zou J, Yu K, Cheng D, Han Y, Zhan J. Plasma application for more environmentally friendly catalyst preparation. Pure Appl Chem 2006;78:1227-38.

[50] Rahman M S, Shaislamov U, Yang J K, Kim J K, Yu Y H, Choi S, Lee H J. Effects of electron beam irradiation on tribological and physico-chemical properties of Polyoxymethylene copolymer (POM-C). Nuclear Instruments and Methods in Physics Research B 2016; 387: 64-62.

[51]Karuppiah J, Linga Reddy E, Sudhakaran M S P, Lee S B. Production of synthesis gas from dry reforming of propane with carbon dioxide over ceria-promoted nickel foam catalysts. RE&PQJ 1(14), 742-747 (2016).

[52] Shang S, Liu G, Chai X, Tao X, Li X, Bai M, Chu W, Dai X, Zhao Y, Yin Y. Research on Ni/g-Al_2O_3 catalyst for CO_2 reforming of CH_4 prepared by atmospheric pressure glow discharge plasma jet. Catalysis Today 2009;148:268-274.

[53] Balcaen V, Roelant R, Poelman H, Poelman D, Marin G B. Catalysis Today, 2010, 157, 49-54.

[54] Zhong Z, Chen K, Ji Y, Yan Q. Methane combustion over B-site partially substituted perovskite-type $LaFeO_3$ prepared by sol-gel method. Appl Catal A Gen 1997;156:29-41.

[55] Rahemi N, Haghighi M, Babaluo A, Fallah Jafari M. Syngas production via CO_2 reforming of methane over plasma assisted synthesized Ni-Co/Al_2O_3-ZrO_2 nanocatalysts with different Ni-loadings. Int J Energy Resource 2014;38:765-79.

[56] Zhou L M, Xue B, Kogelschatz U, Eliasson B. Energy Fuels 12 (1998) 1191.

[57] Ce Li, Brown T C. Carbon oxidation kinetics from evolved carbon oxide analysis during temperature-programmed oxidation. Carbon 2001;39:725-32.